Annals of Arid Zone 52(3&4): 181-207, 2013

Quantification of Aeolian Bedform and Process Parameters in Thar Desert for Earth Surface Dynamics

Amal Kar*

ICAR-Central Arid Zone Research Institute, Jodhpur 342 003, India

Abstract: Aeolian geomorphology, like other branches of geomorphological research, has undergone a gradual change over the past half a century, especially as digital revolution, access to various remote sensing products and sophistication in instruments for measurement have enabled perception and visualization of the bedforms and processes in such quantitative details that were never possible earlier. Small, compartmentalized, site-based studies devoted to one or two identified aspects are now getting replaced by wide-field, multi-disciplinary approaches for a holistic view of the issues involved in bedform-process interaction, and their relationship with the overall land surface dynamics. Relationships with large-scale atmospheric processes, studies on which were partly neglected during last few decades, are now being investigated in greater details, providing exciting new perspectives, or validating some old ideas. Since human beings have become a major driver of change in the sandy landscape, integrated analysis of bio-physical and social aspects are also getting due importance. Quantification of bedform and process parameters, as well as of a host of other linked fields, is a key to this new research. This article reviews and summarizes the aeolian research on Thar Desert in the light of the above developments. It also attempts to draw regional perspectives from the data generated by field-based research, and suggests a way forward.

Key words: Granulometry, wind erosion, sand transport, dune movement, dune formation, dust emission, atmospheric boundary layer, remote sensing, GIS.

Geomorphology is the study of earth's landscapes over time and space, and involves an analysis of both its surface features as well as the processes responsible for their formation and evolution. Historically, the subject evolved through monumental studies on supposed evolution of the landscape, based on intuitive knowledge of researchers on the landscape response to endogenic and exogenic forces, providing visions of possible changes over a time scale of centuries to millennia or more. As older concepts began to be confronted with newer ones, and applied aspects started receiving greater attention, a need was felt for adequate quantification of the features and processes, both fluvial and aeolian. During the past half a century geomorphology has undergone a radical transformation, especially with the advent of digital revolution. Analysis based on quantified parameters is now fast replacing the classical geomorphology that was based largely on power of observation, intimate knowledge of forms and processes and intuitive reasoning, yet fewer measurements. Analysis of earth's land surface dynamics is now more data-demanding, and any hypothesis on land surface evolution (i.e., changes in time domain) or any other kind of interpretation is required to be tested on the basis of quantifiable parameters. This requirement has encouraged instrumentation at critical locations and time, leading to attempts to quantify the rates of changes in landform processes and forms, and then to simulate the changes through laboratory modeling. Quantification of related bio-physical parameters (e.g., atmosphere, soils, vegetation, surface and groundwater) and coupling the changes with those in geomorphic parameters have helped to improve our understanding of the land surface dynamics. Initially the studies were mostly site-based, data from which were collated and modeled to find out the spatio-temporal changes at local to regional scales. Reliability of up-scaling depended heavily on the distribution and density of monitored sites.

Gradually the measurement and monitoring of several parameters have now been shifted from field stations to pixels from satellite sensors, especially as vast advances took place in digital remote sensing since the launch of the first Earth Resources Technological

*E-mail: akarcaz50@gmail.com
Present address: A-1/6, Baitalik Housing Society, KMDA Housing Complex, Baghajatin, Kolkata, India

Satellite (ERTS-1) in 1979. Improvements in our knowledge of the sensor-derived properties of atmosphere and landscape, and progress in calibration of the pixel products through matching with the quantified parameters from field-monitoring sites help us to determine the spatial accuracy of measured products by resolution of the individual pixels. Since many of the satellite sensors collect data at hourly, daily or several days' intervals, and at different pixel resolutions, the scope for measuring many of the fluxes at local to regional scales has greatly increased. Indeed, there already exists a large repository of various global land surface parameters at daily to monthly intervals. This has opened up numerous possibilities of looking at the system response to different pressures. Meaningful integration of the data from atmosphere, geosphere, hydrosphere and biosphere (which together can be loosely clubbed as the bio-physical dataset, where the biosphere is often restricted to the non-human components) with the data from 'human system', or the socio-economic realm, will help to understand the system mechanism better and to address resolving of problems with more confidence. We propose to discuss the progress in aeolian research on Thar Desert in the backdrop of above developments and possibilities.

Thar Desert Landforms

Situated between the Aravalli Hill Ranges in the east and the Indus River in the west, Thar Desert (~290000 km^2) is dominated by a sandy landscape, and is a part of the western arid zone of the Indian Subcontinent. Its landforms and land-forming processes are influenced by high moisture deficiency and peculiarities of the monsoon circulation, which create conditions favorable for aeolian processes to function more efficiently during the pre-monsoon summer months. Fluvial processes are now more episodic, depending on the strength of the monsoon rains. A slow weathering process continues throughout the time-scales, which assists in sediment production for the major sub-aerial processes to act upon. A significant part of the desert landscape is either dominated by faceted slopes and stretches of rocky/gravelly pediments, or is buried under sand and colluviums/alluvium. There are, however, many areas within the desert with thick fluvial deposits, which could not have been formed by processes operating under dry climatic conditions like those of today. The dominantly fluvial landform sequence here is: hills and uplands (also Hamadas) - rocky/gravelly pediments (and pavements) - buried pediments (colluvial plains) - flat older alluvial plains - younger alluvial plains - river beds. Monsoon vigor and past courses of the large perennial Himalayan streams like the Sutlej contributed much to the fluvial and fluvio-lacustrine sedimentation in the region, but drier climatic interludes and tectonic activities put a limit to their occurrence and efficiency (Kar and Ghosh, 1984; Kar, 2013). Throughout the Quaternary period and even before it, whenever the aeolian processes dominated over the fluvial landscape, a new set of landforms was sculpted, especially as sand sheets, sandy hummocks and sand dunes. As a result aeolian sand has now an almost ubiquitous presence in the landscape of not only Thar Desert (Kar, 1993, 2014) but also in the landscape along its fringes in the north (southern parts of Punjab and Haryana; Naruse, 1985), south (north Gujarat; Juyal *et al.*, 2003), and east (east Rajasthan; Goudie *et al.*, 1973). The outer limits of the relict aeolian features beyond Thar Desert define the boundary of a Megathar that existed during past periods of higher aeolian activities.

Multiple evidences from morphological characteristics, stratigraphy and sediment dating reveal that climatic oscillations between dry and wet phases continued throughout the Quaternary period, and even before it, which led to the relative dominance of fluvial and aeolian processes (Ghose *et al.*, 1977; Kar, 1995, 2014). Signatures of definitive pre-Quaternary aridity in the region can be traced to as early as the late-Jurassic Bhadasar Sandstone sequence in which aeolian sand beds, impregnated with innumerable ferricreted nodules, occur as near-shore deposits. Stratigraphic and luminescence studies on the late Quaternary deposits suggest that during the last ~160 thousand years (kilo annum; ka) major pluvial periods in our desert were ~126 ka, ~90-80 ka, ~55 ka, ~30 ka, and 7-6 ka, while the major periods of enhanced aeolian sand mobilization (and possibly a transition to/from full monsoon strength) were ~160 ka, 115-100 ka, 75-65 ka, ~50 ka, 30-25 ka, 14-7 ka, 5-3 ka and 2-1 ka. Significantly, the Last Glacial Maximum (LGM; 24-18 ka), which was the driest period in the region during last

100 ka, did not experience high sand accretion and dune development, possibly because of weak monsoon winds during cooler climatic phases. Much of the dune building activities took place after a major dry phase was over and the monsoon winds started building up over the region. Dune building activities dwindled when vigorous monsoon phases prevailed (Kar *et al*., 2001, 2004; Dhir *et al*., 2010). This is analogous to the present-day conditions when sand reactivation begins with the increasing strength of the seasonal pre-monsoon wind from March onwards and declines when the monsoon rains arrive in mid-June to early July (Kar, 2013).

Unfortunately, dating of the sediments did not help in establishing any rates of processes in the past, except at one transverse dune site in western Thar where dating of the sediments and measurement of the advancement of palaeo-crests of the dune revealed a vertical accretion rate of ~0.61 cm a^{-1} during 2.1-1.9 ka, when dune crest advanced by ~0.87 m a^{-1}. Between 1.8 ka and 0.58 ka the accretion rate declined to 0.08 cm a^{-1} and crestal advancement rate to 0.25 cm a^{-1}. Since then the vertical accretion rate is >2 cm a^{-1} and crestal advancement rate 1.5-9.0 cm a^{-1} (Kar *et al*., 1998, 2004). The unavailability of such data from other parts of the desert is primarily because of the sampling and dating strategies in the project that focused heavily on selecting sites for establishing antiquity of the fluvial and aeolian episodes and deciphering their major periods of occurrence (hence a search for few representative deep sequences, and sacrificing search for adequate number of shallow dune profiles of recent origins). The other major reasons for missing out on rates of aeolian processes were large-scale homogenization of sediments in the older aeolian deposits, limitations of the methods to date sediments with some reliability between ~0.3 ka and 150 ka, and large error margins associated with any single date. On hind-sight one feels that the above factors have severely restricted the utility of the dates to academic discourse on outlines of the past environments. Much of the present-day changes in sandy landscape are confined to the events of past 1-2 centuries, and more to the past 6-7 decades, when human pressure and technological revolutions have prompted large-scale land use changes in the sandy landscape, encouraging higher reactivation and mobility of the bedforms. Unfortunately, this historical period is difficult to date reliably with the methods adopted. The dates on our desert sediments and the deduced environments sketch the broad first-level framework of late Quaternary period.

Based on the dominant landscape assemblages, seventeen major geomorphic provinces (GP) can be identified within the desert, most of which are dominated by dune fields (Fig. 1). Broadly the dune fields cover about 61% of the total area, while the major sandy plains cover 25% area and major rocky/gravelly surfaces the rest 14% (Table 1). Parabolic dune fields cover the largest area, but the linear and transverse dune fields also cover significant areas (Kar, 2014). Details of landforms in the arid western part of Rajasthan, mapped through a new method, are provided by Moharana *et al*. (2013). Aeolian sand is ubiquitous, even on the rocky/gravelly units, and signifies the continued pre-eminent role of summer wind as a major driver for fashioning the landscape. This is despite the fact that wind strength has gradually declined during the second half of the Twentieth Century at many stations, except a few notable periods of increased strength (Fig. 2 and 3). Such falling trend has been noticed at many stations across India and in northern hemisphere, and hence this could be considered a global phenomenon (Vautard *et al*., 2010; Zhao *et al*., 2011; Singh *et al*., 2011; Jaswal and Koppar, 2013). An increase in wind strength has been noticed at some stations since the beginning of this century. GCM data suggests that the trend of increasing strength of the wind in the desert may continue throughout the present century (Kar, 2012). The long-term mean annual pattern of wind at different stations in the desert and the dominant wind vector during June provide a broad idea of the timing and pattern of sand re-distribution across the desert as well as their likely influence on aeolian bedform development (Fig. 4).

Site-based Quantification of Aeolian Bedforms and Processes

The major challenge in Thar Desert is quantification of the aeolian process-form interaction. Despite the fact that sand dune and other sandy bedforms dominate our desert

Table 1. Major geomorphic provinces (GP) in Thar Desert

GP code	Name	Area (km²)	% area
1	Aravalli hills and piedmonts with/without obstacle dunes	12550	4.3
2	Ghaggar alluvial plain of N	16400	5.7
3	Star dune field of N	1750	0.6
4	Transitional parabolic dune field of NE	46450	16.0
5	Luni alluvial plain with isolated hills and colluvial plains	41840	14.4
6	Siwana hills with obstacle dunes	1850	0.6
7	Transverse dune field of NW	17800	6.1
8	Parabolic dune field of NW	11550	4.0
9	Hamada landscape of Jaisalmer with sand streak and zibar	6800	2.3
10	Gravel pavements with isolated sand dunes and sand streaks	17350	6.0
11	Parabolic dune field of S	54950	18.9
12	Nagarparkar upland	1050	0.4
13	Saline alluvial plain of NW	14650	5.1
14	Transitional parabolic dune field of NW	6760	2.3
15	Rohri upland	900	0.3
16	Network dune field of W	17250	5.9
17	Linear dune field with megabarchanoids in W	20100	6.9
	Total	290000	100.0

landscape, and wind erosion is an important problem to tackle, quantitative studies on aeolian process-form interactions are not many. This is especially because of the lack of proper instrumentation and logistics for simultaneous measurement of several atmospheric, topographic and sedimentary parameters during the hot summer months of March to

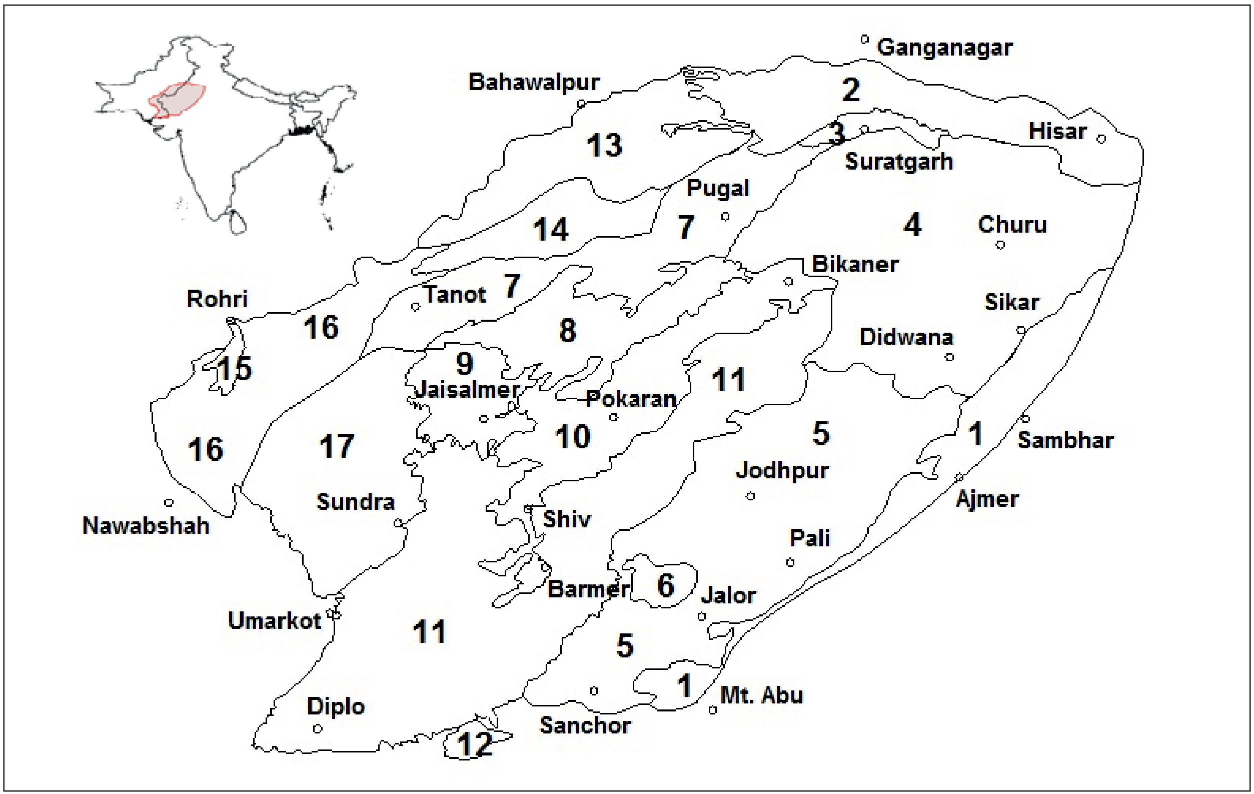

Fig. 1. Geomorphic provinces in Thar Desert. Numbers in the map refer to provinces in Table 1.

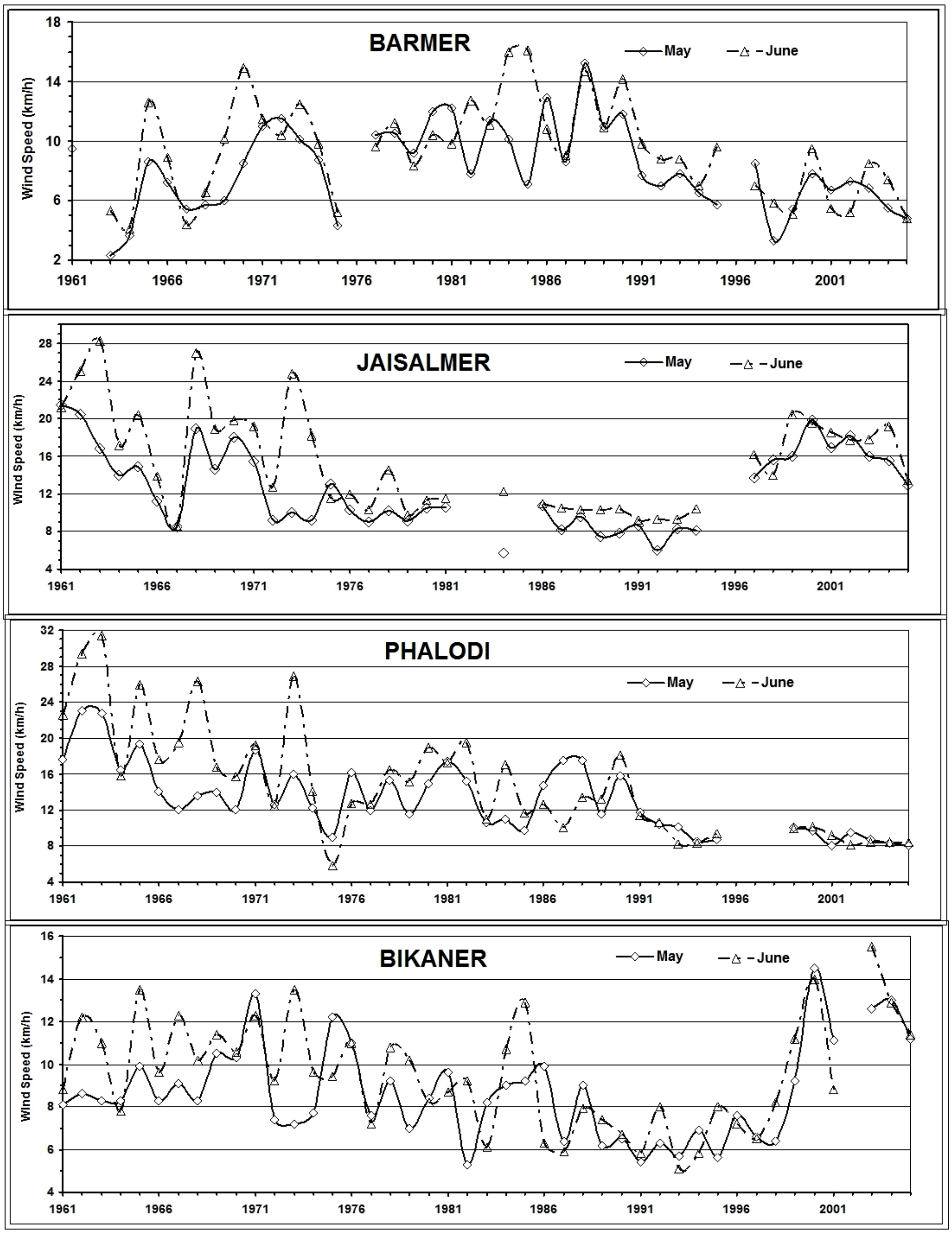

Fig. 2. Mean wind speed for May and June (1961-2005) at IMD stations Barmer, Jaisalmer, Phalodi and Bikaner.

June when the processes become active. The relationships among the variables are also more complex than in a fluvial environment, and vary with the horizontal and vertical components of the flux.

Granulometry of aeolian landscape

In order to find out if there is distinctive granulometric signature of different types of aeolian bedforms in Thar Desert, we carried out some studies on the nature of variation in the distribution curves and central tendencies of grain size, using methods proposed by Folk and Ward (1957). In Jaisalmer District in the west, a broad agreement was noticed between the mean grain size characteristics and the dune types and their activation state (Kar, 1990, 2002). Dry sieving of about 800 carefully sampled near-surface sediments from different landforms in the Indian part of the desert (sampling depth: 10-30 cm for recent sand deposits; 60-90 cm for older deposits), including the crest of different

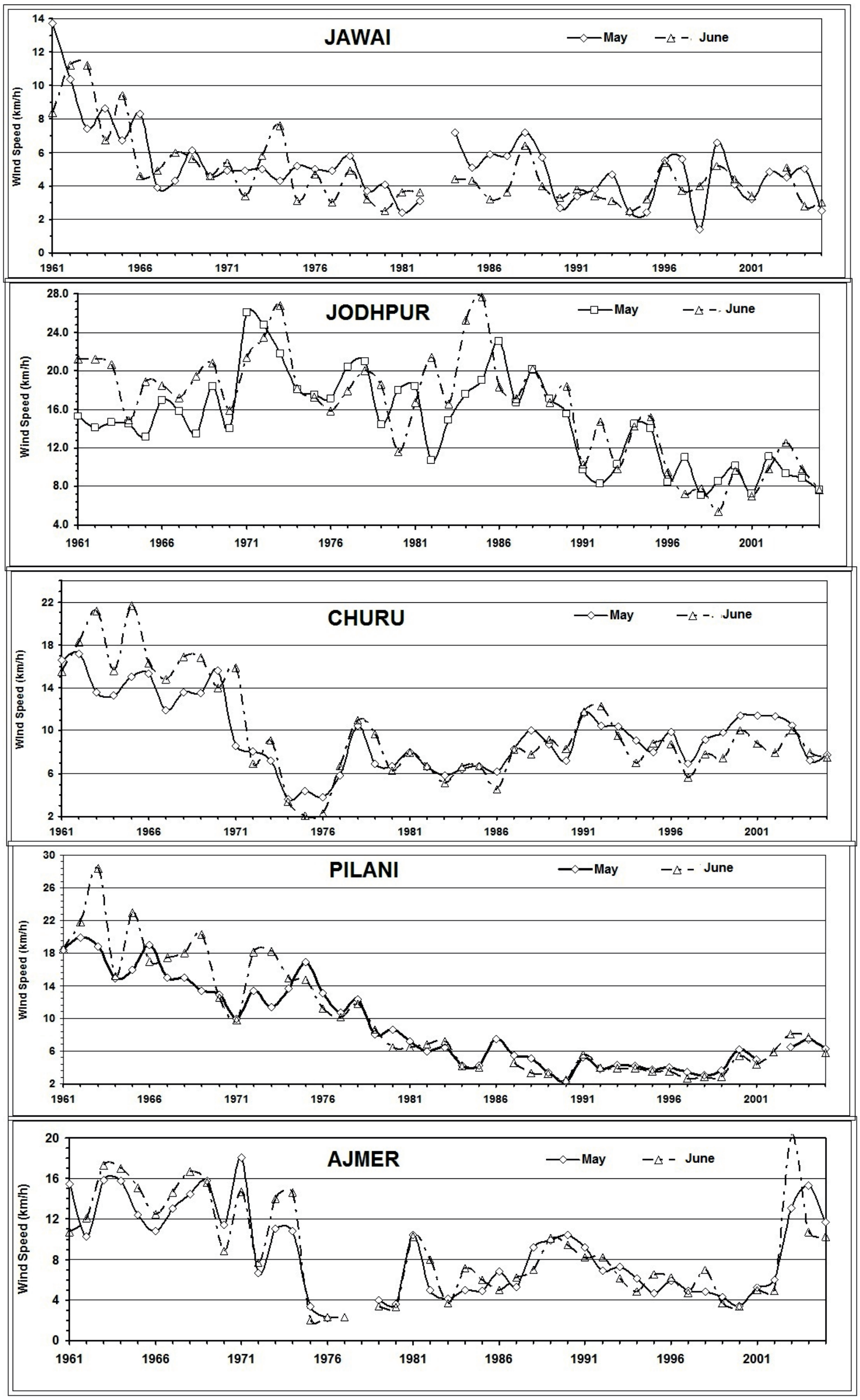

Fig. 3. Mean wind speed for May and June (1961-2005) at IMD stations Jawai, Jodhpur, Churu, Pilani and Ajmer.

dune types, reveals a preponderance of fine to very fine sand in all the dune types. Almost all the crescentic new dunes and most of the reactivated old dunes have fine sand (250-124 micron; 2-3 phi) at their crests (>90% of samples reporting), while 65-70% samples from

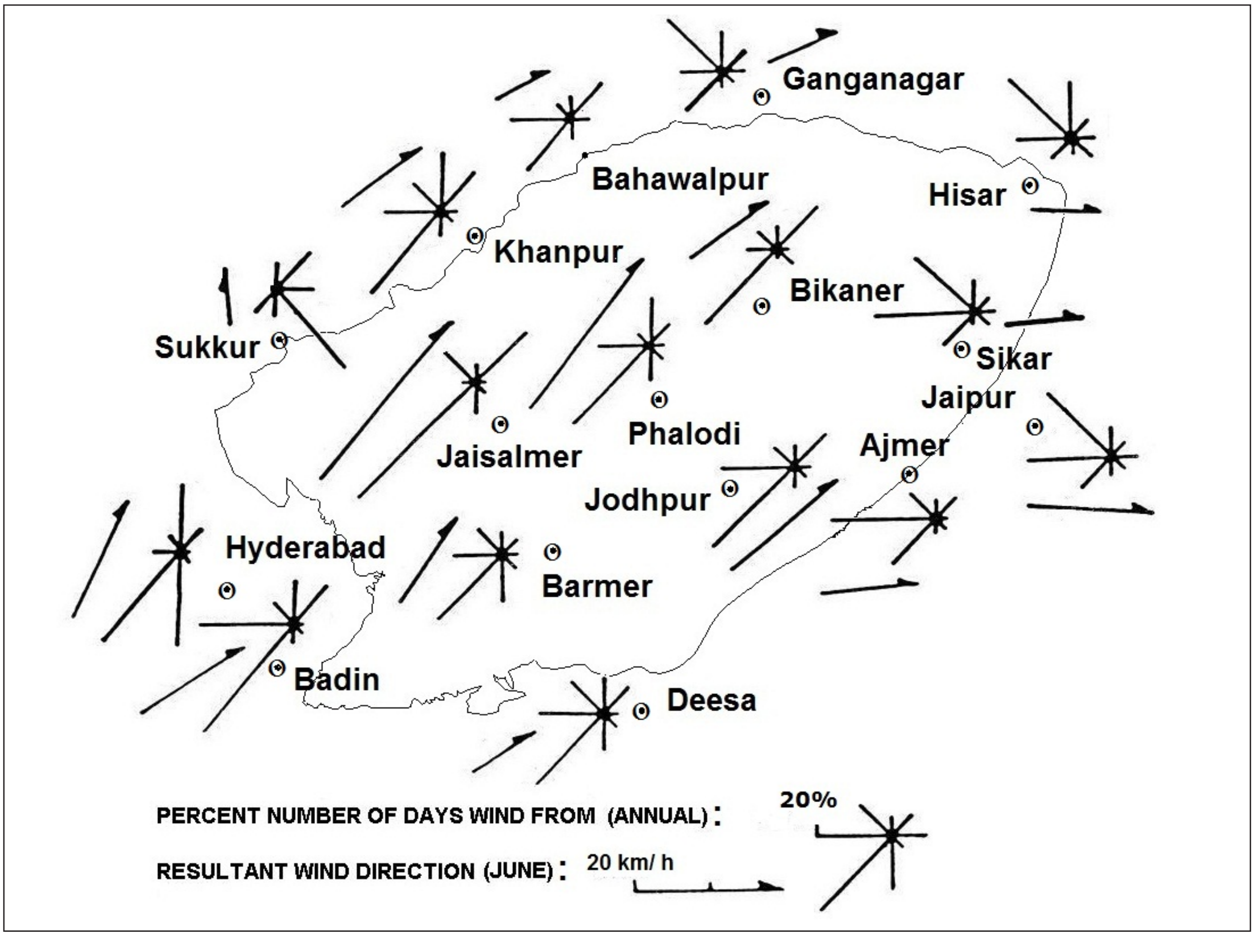

Fig. 4. Mean percentage number of days wind from different directions (annual), and the mean resultant wind direction (June) at stations in and around Thar Desert.

the crest of non-crescentic new dunes and from the stable crests of old dunes have a dominance of fine sand, the rest having a dominance of very fine sand (125-63 micron; 3-4 phi), but also some medium sand (500-250 micron; 1-2 phi). About 60-70% samples of star dunes and transitional parabolic dunes have a dominance of very fine sand, as they occur nearer to the northern alluvial plains where ~12% samples are dominated by coarse silt (63-16 micron; 4-6 phi). Broadly, fine sand dominates in the near-surface sediments of the sandy plains across the desert within India (average 66-86% in different geomorphic provinces), but relatively lower average values are noticed in the northern alluvial plain and the transitional parabolic dune field of NE (<70%), where silt constitutes 20-30% of the total weight. Elsewhere, the sandy plains usually have 2-5% silt in the near-surface layers, except in the northwest, where the content increases to 6-7%. Crestal sediments of sand dunes, both old and new, have 1-2% of silt in large areas, except in the NE and NW where the content increases to 4-5% due to the silt-rich alluvium on which the dunes occur. The zibars and the nebkhas have 8-12% of coarse to medium sand, while the obstacle dunes have about 6% medium sand. The near-surface layer of the dry Ranns has about 7% silt and 6% coarse to medium sand. Such spatial distribution of near-surface sediment size has implications for sand movement and dust emission.

Most dune crests have a dominantly unimodal distribution of sand. The crest of the 25-40 m high megabarchanoids and the taller barchans (mostly 5-8 m high) consist exclusively of unimodal fine sand that is well to very well sorted (S= 1.41 or less). Bimodality has been noticed in the low dunes like the zibars and the nebkhas. Many of the high old dunes, especially in the linear dune field in the high wind-energy zone to the SW of Jaisalmer and in the adjacent parabolic dune field (including the hair-pin parabolic dunes) and the transverse dune field, have also bimodal sand. Bimodality of crestal sand has also been reported from several other deserts (Ahlbrandt, 1979; Thomas, 1986; Watson, 1989). Bimodal and even polymodal distribution of grains is common in sandy plains due to parent material variability and frequent admixing of aeolian and fluvial transportation of grains.

Explanation for bimodality of sand: Warren (1974) suggested that "when the medium-sized sand in a poorly sorted mixture is moved by the wind it bounces off the coarser grains on the surface and moves quickly downwind, whereas the fine sand can lodge between the coarser grains and be protected there from further bombardment". This appears to partly explain the distribution, but the occurrence of a secondary peak or a high bench of very fine sand population can be partly due to a fall of the suspended load during the cessation of any single gust of wind within a sandstorm. Apparently the process gains prominence in areas where the adjacent sandy plain or interdune plain has higher amounts of very fine sand and silt. During any sandstorm the fine sand and silt from such plains are carried up the dune slopes with gusts, and much of the load is released at or near the dune crest as soon as the gust falls. Although coarser grains do also travel fast to the crest through saltation during gusts, the stronger wind force at the crest as a result of higher speed up ratio from the windward base cannot possibly winnow out all the finer particles that get collected at the cessation of previous gusts. Possibly the fine particles get trapped in between the voids of other medium to coarse particles there to create a secondary peak or a bench. This mechanism of smaller particles falling in between the interstices of larger particles is called 'sifting'.

Increased sediment flow during gusts has also been noted from the Australian Desert where Folk (1971) suggested that the sediments arrived at the dunes as quanta, related to the individual gusts. Similar mechanism was also suggested for the bimodal sand in transverse dunes of Arabian Desert (Vincent, 1984). Surprisingly, many of the transitional parabolic dunes in the much lower wind-energy environment of north-eastern Thar (as hooked dunes in Didwana-Sikar-Churu area or as wide and disjointed parabolic arms with smaller linear and transverse bedforms in between the bounding arms) and the very old and partly gullied, 'fossilized' parabolic dunes in the upper Luni plains along the eastern fringe of the desert (Govindgarh-Pushkar area) also have such distinctly bimodal sand at their crest. The latter area has several instances of tri-modal sand also at the crest. In all the above instances of bimodal sand, from west to the east, the sand grains are moderately well to very well sorted. If the process of bimodality suggested in the previous paragraph is valid, then it is likely that the same process is acting over the dunes in the east also, though at a much slower pace. The tri-modality at the crest of fossilized parabolic dunes could possibly be due to a new influx of aeolian sand from the adjacent Luni plains over a crest where bimodal sand from a previously active phase remained dormant for a fairly long period.

Patterns of central tendency: The average values of mean (Mz) and median (Md) grain sizes in the crescentic dunes together (barchans, barchanoids and megabarchanoids) are almost identical (2.69 phi), with an average sorting coefficient (S) of 0.383. The average finest Mz (2.78 phi) and Md (2.77 phi) among the three types are seen in the barchans, but this is an artefact of spatial averaging over different provenances. Barchans were sampled over a wide range of sandy plains, and included those on deep fine alluvium to the ones on very shallow colluviums. Barchans along the eastern fringe and northern plains occur on fine alluvium and have the finest average Mz (3.04 phi) and Md (3.01 phi), where average S is 0.421. In the shallow sandy plains of Jaisalmer-Ramgarh area the average values become 2.52, 2.54 and 0.423, respectively, while over the central sandy plains the averages become 2.71, 2.71 and 0.356, respectively. The non-crescentic new dunes (zibars, nebkhas and source-bordering dunes) have average Mz and Md of 2.86 phi and 2.89 phi, respectively, with S of 0.620. The old dunes with relatively stabilized crests have average Mz and Md of 3.04 phi and 3.03 phi, respectively, with S of 0.475, while those with reactivated crests have average Mz of 2.85 phi, Md 2.82 phi and S 0.386 (Table 2).

We presumed that the process of sand shifting along the slope of a small barchan or a tall megabarchanoid is the same, which apparently should leave a similar signature of change in central tendency values along the windward slope of the two dunes to their crests. We, therefore, examined the Mz, Md and S values along the slopes of barchans and the megabarchanoids. In the case of barchan, the samples were collected at Selvi (near Pokaran) from (a) the path of an aeolian streamer upstream of the barchan (detailed in a subsequent section), (b) a narrow rim of coarse ripples slightly upwind of the barchan foot slope, (c) barchan foot slope, (d) lower mid-slope of the barchan, (e) mid-slope of the barchan, (f) barchan crest, (g) mid-slope of the slip face, and (h) near the base of the slip face (Fig. 5). In the case of megabarchanoid, we collected the samples from a megabarchan segment in the generally inaccessible Makne ka Tar area (S of Shahgarh), the sites being (a) lower mid-slope of the megabarchan, (b) dune crest, (c) mid-slope of the slip face, and (d) near the foot of the slip face (Fig. 6). We find that as the wind carries sand up the windward slope of a barchan, it progressively grades the sand and sorts it, such that both Mz and Md become finer and S better till the crest is reached. At the crest the grains suddenly become much coarser and sorting gets poorer, which persist to the brink. The grains become finer again along the slip face; the finest Mz and Md occur at the base of the slip face. An almost identical situation is found in the case of the megabarchan segment, suggesting that despite the large difference in dune height, wind environment, sediment provenance and flux, the process of sand mobilization and sorting is similar on both the types, and presumably over the barchanoids (6-15 m height) also. Such behaviours of sand grains along the slopes of crescentic dunes have also been reported from other areas (Bagnold, 1941; Barndorff-Nielsen *et al*., 1982). Laboratory simulation by Sarr and Chancey (1990) suggests that as a sand grain at the crest is bombarded by the

Table 2. Average central tendency of near-surface sediments from sandy plains and sand dunes in the Indian part of Thar Desert

Major Landform: Type	Sub-type	Mean phi	Median phi	Sorting	Skewness	Kurtosis
Sandy Plains (colluvium/ alluvium/interdune)		3.15	3.19	0.814	-0.027	1.648
	Colluvial Plain	2.80	2.87	0.934	-0.101	1.791
	Alluvial Plain	3.75	3.73	0.651	0.106	1.487
	Interdune Plain	3.14	3.16	0.726	-0.012	1.591
Sand Dunes (New bedforms)		2.77	2.79	0.501	0.009	1.197
	Zibar	2.73	2.86	0.825	-0.191	1.491
	Source-bordering	2.93	2.92	0.491	0.068	1.254
	Nebkha	2.91	2.89	0.544	0.092	1.232
	Sub-total: Non-crescentic	2.86	2.89	0.620	-0.010	1.326
	Barchan	2.78	2.77	0.396	0.041	1.156
	Barchanoid	2.66	2.66	0.379	0.042	1.022
	Megabarchanoid	2.63	2.63	0.373	0.000	1.026
	Sub-total: Crescentic	2.69	2.69	0.383	0.028	1.068
Sand Dunes (Old bedforms)		2.92	2.91	0.430	0.091	1.247
	Stable dune crest	3.04	3.03	0.475	0.046	1.259
	Reactivated dune crest	2.85	2.82	0.386	0.131	1.269
	Linear	2.79	2.78	0.431	0.051	1.325
	Parabolic	2.86	2.85	0.372	0.096	1.302
	Transitional Parabolic	3.01	2.99	0.435	0.116	1.181
	Complex	3.06	3.05	0.588	0.063	1.459
	Transverse	2.88	2.88	0.355	0.055	1.173
	Star	3.05	3.02	0.517	0.108	1.065
	Thal	3.43	3.45	0.463	-0.044	1.229
	Obstacle/Echo	2.87	0.50	-0.073	1.306	2.907

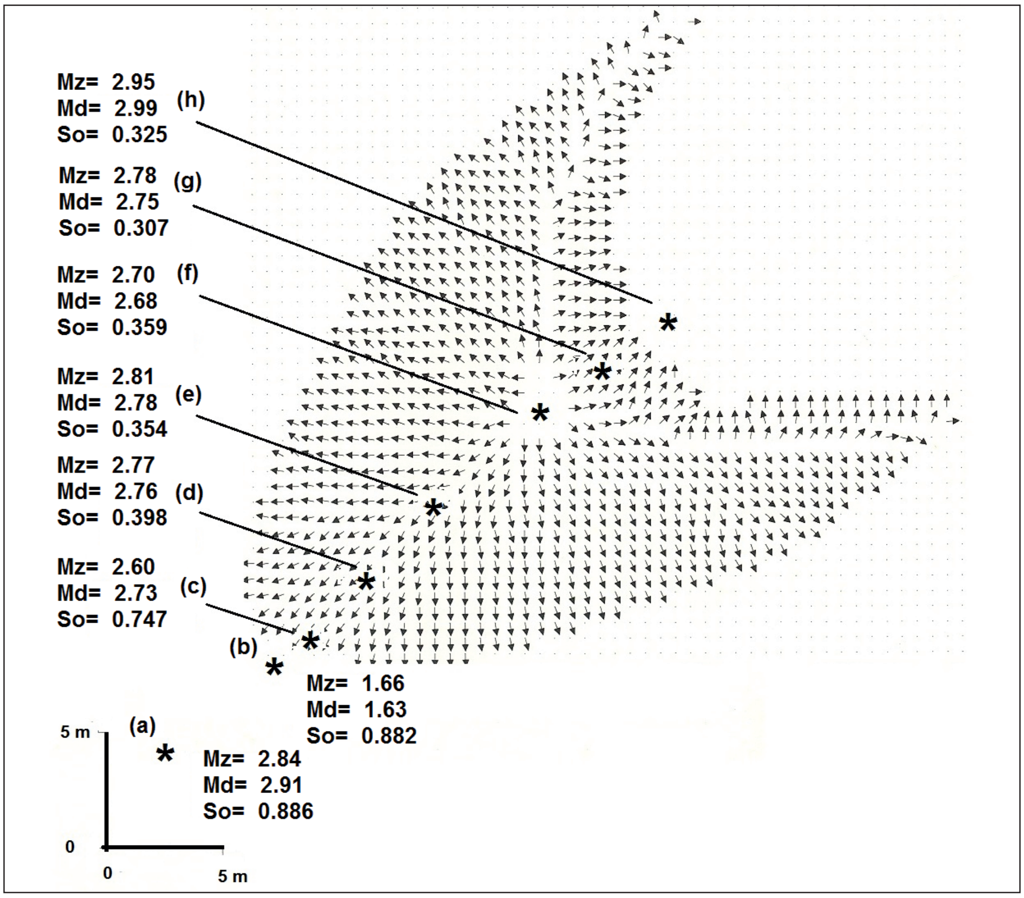

Fig. 5. Mean (Mz), median (Md) and sorting coefficient (S) of grain size along a barchan at Selvi near Pokaran. Sites (a) to (h) are as given in text.

saltation impact it is first pushed downward, but soon the grain gets resistance and, hence, bounces back to the surface. A compressional wave propagates from the target grain into the underlying grains and during this stage the grains are in continuous contact with their surroundings. Behind the compressional wave is a rarefaction wave in which the grains lose contact with their immediate surroundings and move up, as well as move horizontally forward.

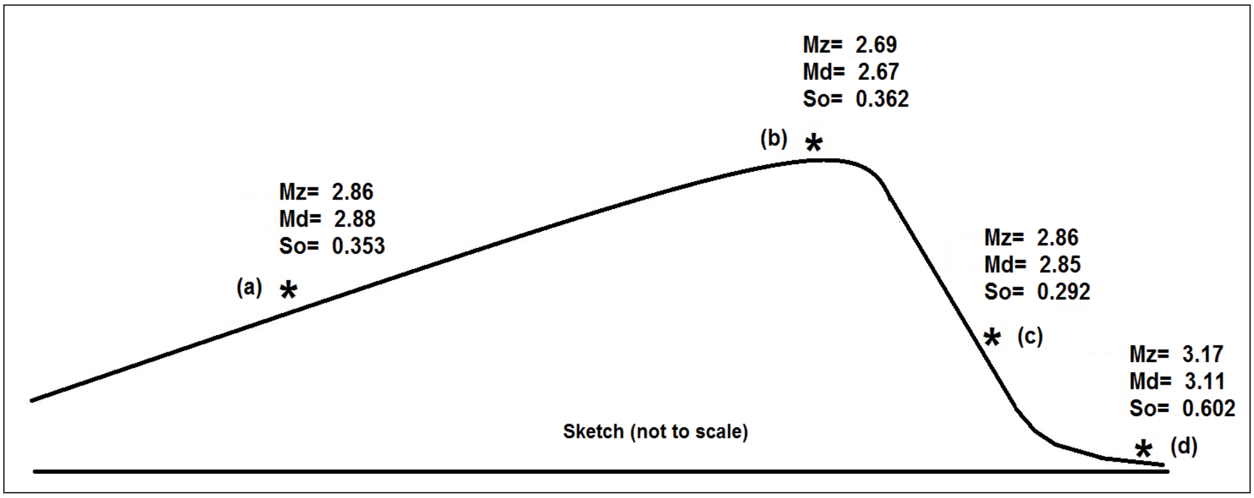

Fig. 6. Mean (Mz), median (Md) and sorting coefficient (S) of grain size along a megabarchan at Makne ka Tar near Shahgarh. Sites (a) to (d) are as given in text.

The coarser grains in the mixture rise more and get ejected more by rotating and ratcheting themselves against the smaller ones. With increased ejection speed the reptation/creep at the crest is replaced by saltation.

Grain size generally becomes finer with antiquity of the surface deposits because erosion exposes the partly pedogenized sub-surface layers and dust-fall also enriches the surface. Sorting, however, gets poorer with stability, as a slow creep tends to mix the previously sorted sediments. Poorer sorting in zibars and nebkhas (average S = 0.814) is essentially due to their low height that allows mixing of sand from sandy plains easier through creep and reptation. Broadly, the average characteristics suggest well to very well sorted, symmetrically distributed, leptokurtic arrangement of sand in most dune types, some notable deviations being in the zibars (moderately sorted, coarse skewed), the barchanoids and megabarchanoids (mesokurtic), the transitional parabolic dunes in the NE (fine skewed), and the star dunes (moderately well sorted, fine skewed and mesokurtic). The colluvial plains have moderate to poorly sorted and coarse-skewed grains that are very leptokurtic.

When seen in different geomorphic provinces, the finest Mz and Md in new dunes are found to occur in the linear dune field with megabarchanoids (3.42 and 3.41 phi, respectively), but the old dunes have coarser Mz and Md (Table 3). This is especially because the megabarchanoids and barchanoids have been formed mostly over the deep Saraswati alluvium that was traced below the sand thickness to the extreme west of Jaisalmer District (Ghose *et al.*, 1979), as well as the proximity of the field to the Indus plain. Other sand dunes have been formed over a variety of landscapes that have some control on the supply of sediments to the dunes. Finer Mz and Md on dune crests are also noticed in the NE and NW (spatial averages for both values being 3.00 phi or higher) due to the deep alluvium on which the dune fields occur. Cluster analysis of grain size statistics and dendrograms prepared for their hierarchical grouping almost replicated the type of genetic linkages that one expected (Kar, 1999). Some notable studies in other deserts have also shown the controls of granulometry on dune types and geometry (Wilson, 1972; Wasson and Hyde, 1983; Lancaster, 1995; Thomas, 1988).

Estimates of Sand and Bedform Movement

Field measurements: As has been mentioned earlier, large-scale sand movement in Thar Desert takes place during March to June. If the monsoon rains get delayed or fail as a result of vigorous westerly winds, sand mobility continues till July. Some field measurements of sand movement have been reported in the context of soil erosion under different land use practices. For example, Gupta (1993) reported a loss of 1449 t ha^{-1} top-soil from a bare sandy plain at Bikaner during April to June, 1990, while the loss from a crop field with pearl millet stubbles during the same period was 22 t ha^{-1}. Sandy soil of Bikaner was found to be more prone to erosion (273.7 kg ha^{-1} d^{-1} under a mean wind speed of 20 km h^{-1}) than the loamy soil with numerous clods at Jodhpur (15.6 kg ha^{-1} d^{-1} under the same wind regime). Under the same wind regime a sandy soil with grass clumps at Chandan near Jaisalmer lost 76.7 kg ha^{-1} d^{-1} (Gupta, 1993). Santra *et al*. (2010) estimated a loss of 389 kg ha^{-1} soil at Jaisalmer during a severe sandstorm on 15 June 2009 that lasted for only 30 min. At a regional scale, Dhir (2003) estimated a mean soil loss of 2837 t ha^{-1} from disc-ploughed sandy soil during a 22-day-long sandstorm across the western part of the desert in 1985, when the loss from conventionally tilled land was 932 t ha^{-1}, that from long-fallow land with small shrubs/weeds 207 t ha^{-1}, and from degraded pastures 472 t ha^{-1}. Such losses have been found to affect the soil fertility status (Raina, 1992), which is already poor compared to that in the adjoining semi-arid plains. It emphasises the need for proper monitoring of status and causal factors of wind erosion, including the nature of aeolian dynamics over various bedforms and under different uses/covers in the vast desert terrain. This also calls for adequate quantification of the atmosphere-bedform interaction patterns for a proper understanding and large-scale simulation of sand mobility and dust emission scenarios.

Very few studies have been carried out on the mobility of sand and sand dunes in natural landscape and on the behaviour of some key atmospheric variables during the period of

Table 3. Mean phi (Mz), median phi (D50) and sorting coefficient (S) of near-surface sediments from sandy plains and sand dunes in different geomorphic provinces

Geomorphic province	Parameter	Sandy plains	New sand dunes	Old sand dunes - reactivated crest	Old sand dunes - stabilized crest
Aravallis	Mz	-	3.03	2.91	2.94
	D50	-	3.02	2.94	2.95
	S	-	0.363	0.504	0.452
Alluvial plain-N	Mz	3.68	3.11	3.14	3.25
	D50	3.68	3.04	3.09	3.21
	S	0.666	0.527	0.509	0.557
Star dune field-N	Mz	3.19	2.92	2.86	3.16
	D50	3.16	2.83	2.82	3.15
	S	0.678	0.468	0.405	0.607
Transitional Parabolic dune field-NE	Mz	3.51	3.03	2.87	3.01
	D50	3.50	2.97	2.82	2.99
	S	0.706	0.512	0.468	0.420
Luni alluvial plain-S	Mz	2.95	3.00	2.92	2.91
	D50	3.00	3.01	2.96	2.90
	S	0.579	0.531	0.367	0.421
Siwana hills	Mz	3.05	2.99	2.99	2.85
	D50	3.01	3.01	3.01	2.85
	S	0.757	0.302	0.272	0.389
Transverse dune field-NW	Mz	3.40	2.74	2.83	2.95
	D50	3.36	2.71	2.83	2.94
	S	0.485	0.448	0.348	0.469
Parabolic dune field-NW	Mz	2.93	2.79	2.80	2.79
	D50	2.92	2.74	2.76	2.83
	S	0.620	0.368	0.326	0.500
Upland-Hamada-W	Mz	2.58	2.70	2.66	2.94
	D50	2.85	2.75	2.77	2.92
	S	1.117	0.488	0.340	0.316
Pavement-Pediment-C	Mz	2.86	2.71	2.82	2.82
	D50	2.90	2.72	2.79	2.78
	S	0.889	0.434	0.301	0.339
Parabolic dune field-SC	Mz	2.39	2.57	2.80	2.84
	D50	2.52	2.62	2.79	2.82
	S	1.089	0.474	0.295	0.367
Linear-Megabarchanoid dune field	Mz	2.54	3.42	2.69	2.92
	D50	2.73	3.41	2.68	2.89
	S	0.935	0.465	0.440	0.443

mobility. Despite the constraints of getting ideal windy conditions during periods of every measurement, we found that wind speed increases with height along the windward slope of a sand dune and falls sharply in the lee of the dune, along with a change in speed up ratio in that direction (Fig. 7). Over barchans the speed-up ratio from windward base of the dune to its crest during April-June is by 35-50%, which gets translated into the actual transport rate of the sand grains across dune surfaces through reptation, creep and saltation. Trapping of the moving sand at different locations of a barchan during the windy summer month and sand

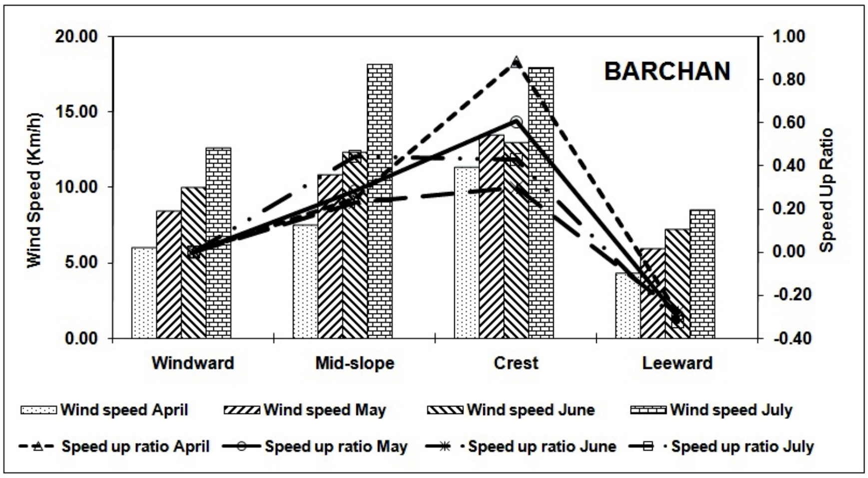

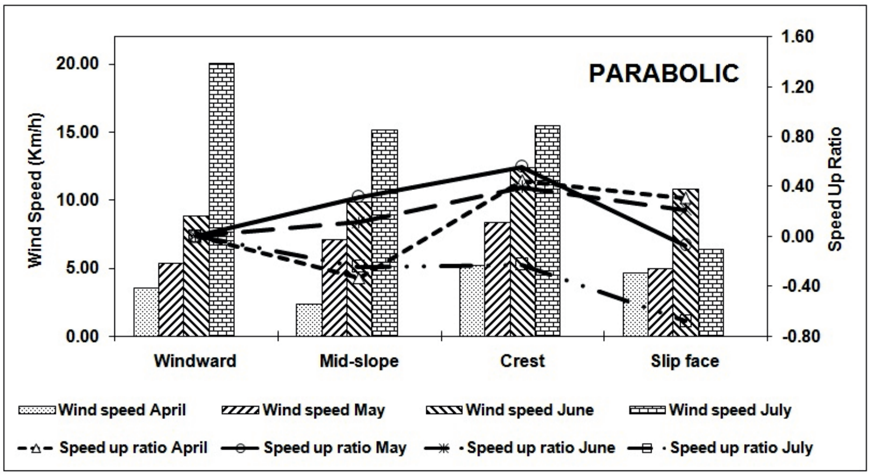

Fig. 7. Wind speed and calculated speed-up ratio (in relation to the speed at windward base) along a barchan and a parabolic dune at Shergarh.

storms showed about 5 times higher flux at the crest than at other parts of the dune. During gusty winds the mean transport rate of fine to medium sand grains (up to 0.2 mm) was measured as 46 kg m^{-2} $hour^{-1}$. A rate of 530 kg m^{-2} day^{-1} was recorded from the crest of a barchan during a particularly windy day (wind speed 6.9 m s^{-1}) in April (Ramakrishna *et al.*, 1990, 1994).

Estimates of sand transport based on fundamental principles

Satisfactory field measurement of aeolian sand mobility and dune movement over the vast desert is a difficult proposition. As a first approximation we used the well-known sand transport equation of Bagnold (1941) to estimate the rates of sand transport at local scales, although some studies show limitations of the Bagnold equations, especially in terms of threshold shear velocity (Dong *et al.*, 2003). Using Bagnold's (1941) equation for sand transport over a flat surface in Pokaran-Jaisalmer area, where the mean sand size of 2.2 phi was kept as an input variable, and the mean wind speed was taken as 39 km h^{-1} (typical for a sandstorm), we estimated a sand transport rate of 195 kg m-width^{-1} h^{-1} (4.68 t m-width^{-1} d^{-1}) on a bare sandy surface. When we integrated this with Wilson's (1971) equation on sand deflation, where the 39 km h^{-1} wind speed was allowed to persist for 20 days, this translated into a potential soil loss of ~187000 t ha^{-1}, or sand deflation to a depth of 9.50 m. If the deflation is restricted to a depth of 20 cm (assuming a hard nodular carbonate layer at that depth) the calculated sediment loss is 3941 t ha^{-1}. Long period of high wind is not very uncommon in the Thar, where strong westerly winds during the pre-monsoon months, especially May and

June, often persist for 15-25 days at a stretch, with gusts of very high winds and smaller periods of relative calm. One such long period of strong wind and sand storm was observed during June-July, 1985. The value of 3941 t ha^{-1} as potential sediment loss agreed well with our field measurement of deflation to a depth of 18-20 cm (mean loss ~3754 t ha^{-1}) in the sandy plain of Chandan during the 20-day-long sandstorm in 1985 (Kar, 1994). Hard carbonate layer at that depth restricted further loss.

To find out sand transport under different plant cover, we then used the Buckley (1987) equation that integrates Bagnold (1941) equation with a wind-tunnel-derived constant and a plant density term. It revealed that under a wind speed of 10 m s^{-1} and a density of 17% cover of grass like *Lasiurus sindicus* the potential sediment loss was ~25500 t ha^{-1} as compared to ~187000 from the bare soil, which means a protection of ~87%. A 4-8% plant cover reduced the transport by 30-50% of that on a bare surface (Kar, 2009). As wind speed increases the efficacy of the plant cover, however, gradually tends to get reduced. There are several other issues of aeolian transport – erosion – vegetation feedback mechanism that also impact the actual aeolian flux in vegetated areas and produce features like pedestalling and street formation, and need proper understanding and quantification for modeling (Okin, 2013).

From sand transport to barchan movement

During the sandstorm of June-July 1985, we carried out field monitoring of a 2.29 m tall barchan over a pediment surface at Selvi near Pokaran, which was experiencing a wind speed of 30-39 km h^{-1}. It revealed a movement of 1.7 m in 3 days. Theoretical calculation with a mean wind speed of 34 km h^{-1} provided a potential sand transport rate of 2.367 t m-width^{-1} d^{-1} on the pediment surface. Thus, in three days the sand transport over the pediment was 7.10 t m-width^{-1}. We then calculated the sand transport along the bare dune slope using the Bagnold (1941) equation: $Q' = Q/ (\cos\theta * (\tan\mu + \tan\theta)$, where Q and Q′are sand transport rates along a flat surface and an inclined plane, respectively, μ is dynamic friction angle for sand, and θ is slope of the surface. We also calculated the rate of advancement of the barchan using the following equation (Wasson and Nanninga, 1986): $c= (QT)/((\cos\theta (\tan\mu + \tan\theta))/\rho h)$, where, c is dune advancement rate, T is sandstorm duration in hour, h is the crest height of the barchan in meters, and ρ is density of the loosely packed sand. These produced a dune advancement rate of 0.027 m, or a movement of 1.99 m in 3 days, which compared well with the field measured movement of 1.7 m, the small variation being largely a result of assumption of a single mean wind speed for an area where the actual weather station was >50 km away at Phalodi (Kar, 1994).

Field monitoring of the Selvi barchan's movement from July, 1987 to June, 1991 showed a travel distance of 190.5 m, with a mean celerity of 32 m a^{-1}. Not all the dune types in the desert move so fast. Even for barchans the celerity in the same wind regime declines with the dune height. As the barchan progressed over a sand-impoverished gravelly pediment, it gradually lost height from 2.29 m in July 1987 to 2.09 by the end of June 1991, apparently because the supply from an upwind source was decreasing with distance. Extrapolating the travel distance and change in height with it, and assuming no change in the environmental determinants of the barchan's movement, we find the possibility of the barchan losing its topographic entity after travelling a maximum distance of ~620 m when the edifice would merge with the sandy plain (Fig. 8). The barchan was also expected to gain some speed with the reduction of height and the mass. Although monitoring the barchan's movement over the years would have been interesting, several new building structures came up along the travel path of the barchan since 1992, which totally deformed its shape.

One would expect from the above that the height of all crescentic dunes should gradually decline as they move forward, but a decade-long observation of some taller barchans (5-8 m high) to the west of Jaisalmer showed no apparent decline in height. Rather, some height gain was noticed. A recent simulation study by Hersen *et al*. (2004) explains this as a result of the ratio of sand flux arriving at dune's upwind end to that leaving the dune at the horns. Although barchans receive a sand flux at their upwind end proportional to their width, the large barchans capture more sand than they lose along the horn tips, as compared to the small barchans. This causes the taller barchans

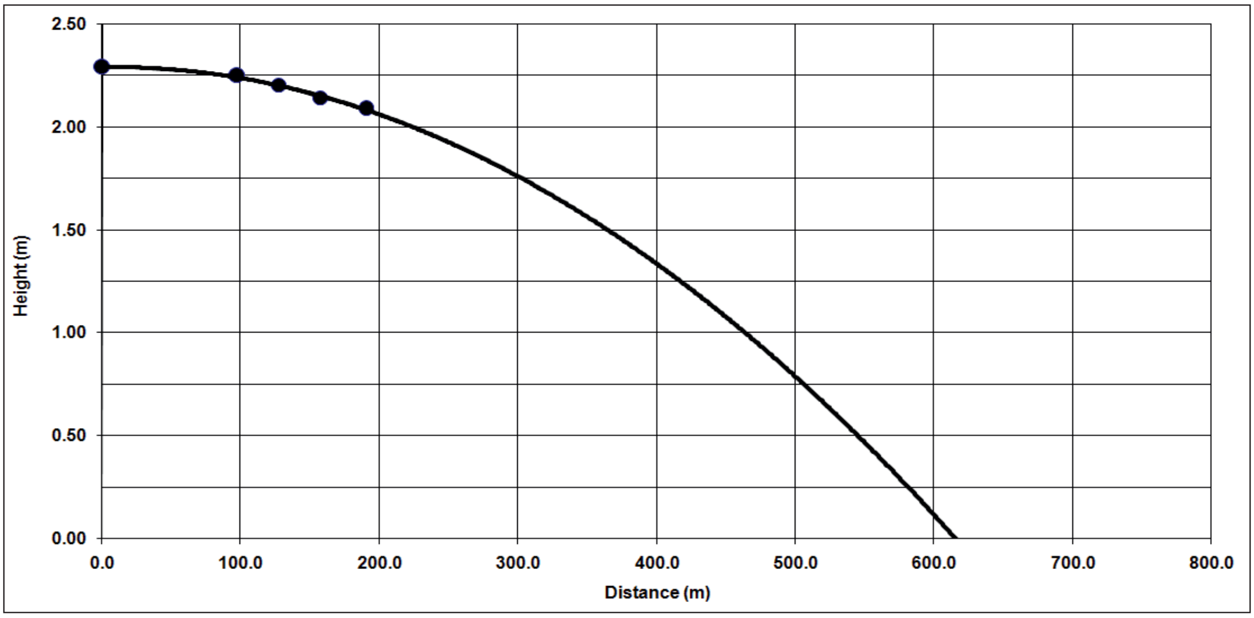

Fig. 8. Measured height and travel distance per year (black dots) of a barchan near Selvi during 1987-1991 and the likely travel distance after which the barchan would disappear under the given circumstances.

to grow in size with time. As we shall discuss later in this paper, such new studies on aeolian bedforms and processes have vastly improved our understanding of the system dynamics. The successful implementation of the barchan mobility equations encouraged us to estimate bulk sand transport pattern over the Selvi pediment and prepare a balance sheet of sand budget in the area under ideal conditions.

Roots of Selvi barchan and modes of sand transport

The measured barchan at Selvi was found to occur on a rhyolite pediment, where several 1-3 m high barchans were moving from SW to NE along a narrow corridor. The source of the sand is ~3 kms upwind near Kelwa where a small ephemeral channel from the surrounding uplands brings enough sand to feed to the aeolian process. A cluster of 1-4 m high barchans were, therefore, formed in this valley segment in an apparently chaotic arrangement. When moving out of this chaotic cluster the individual barchans followed the Selvi route in an orderly fashion and along a narrow corridor. Apparently the change over from a chaotic arrangement of barchans to an orderly fashion of movement was related to a change from the dominantly bulk, roll-over transport mode of the sand to a dominantly streamer mode of transport as the sand-surcharged wind downwind of the valley encountered a higher topography of the pediment that was much impoverished of aeolian sand, hence had lesser sand available for processing and feeding to the barchans. Under such controlled supply of sand, the sand discharge pattern along any individual barchan is expected to be through accretion at the toe of its windward stoss slope and loss through release of streamers at the tip of its two horns (Lettau and Lettau, 1978). This pattern of sand flow around a barchan becomes visible during any period of strong sandstorm over the pediment. Close observations in the area also reveal that the rhyolite terrain downwind of the dry valley of Kelwa is slightly grooved into parallel lanes of relatively lower elevation, which is possibly due to stream-wise sand blasting. These wider lanes, created through the continuation of the blasting process for millennia, should carry the wind faster along them and collect the sand streams within. Observation during many sandstorms in the area helped us to visualize such streamer transport of sand along the barchan lanes.

Estimating bulk transport of sand

Streamer mode of transport along barchan corridor: We calculated the bulk sand transport in Kelwa-Selvi area using Lettau and Lettau (1969) equations. For this, we selected a 2500 m long and 250 m wide barchan-infested strip, which had 16 barchans, spaced at an average distance of 156.25 m. The mean height of the barchans was 2.10 m. Detailed morphometric measurement of the barchans helped us to estimate the area and volume of an average barchan as 384.16 m^2 and 355.87 m^3, respectively. Since the mean density of sand in the locality was 1970 kg m^{-3}, the mean mass of individual barchans was calculated as 701.06 t Further calculations revealed that the volume of sand contained in the barchans in the studied strip, when spread evenly over the plain on which these were moving, could cover an estimated 911.03 mm thickness of the plain. The average streamer length in the corridor (and presumably in the locality as well) was approximately 3.0 km, which implies that if a streamer of sand was released more than 3.0 km upwind of the barchan field, there was more likelihood of it getting dispersed before being available to sustain the barchans here. The total volumetric line discharge of sand (rQ) was found to be 2.91 m^2, and free streamer transport per meter width per year 1.03 m^3. Since an average barchan had a width of 21 m, the expected interception of sand by the barchan in a year was calculated as 21.63 m^3. For all the 16 barchans taken together, the sand interception by barchans was, therefore, 346.08 m^3. In order to maintain equilibrium an individual barchan in the corridor had to release an equal volume of sand from its horn tips. The process should lead to a slow renewal of the sand load being moved along the dune. We calculated the time required by an average-sized barchan in the area to renew its sand load as 16.45 years. The barchan would have to move a distance of 526.40 m before achieving this feat, and roll-over its material 17 times over this distance, before sand renewal could take place. Since the total length of the barchan corridor was 5 km, our calculations suggested that an average-sized barchan would renew its sand load 10 times while crossing this whole length of the corridor. The calculations were based on some simplistic assumptions and averaging of barchan configuration, but provide a procedure to understand in quantitative terms some important steps in the processes of sand accretion and dune movement.

With proper sand budgeting of such areas it may be possible to broadly locate the distance from where a particular barchan cluster gets its supply, and how much. It may also be possible to estimate at what rate the dunes in a cluster should progress with time, and what new areas they would engulf. Answers to these questions would help to effectively control their menace, or to find out ways to convert the adversity into opportunities. Since the beginning of this century, several new modeling studies have provided us with improved understanding of the aeolian bedform-process interaction. Most of these studies have modeled the streamer transport of sand and evolution of barchans, but some studies have attempted the modeling of other dunes also (Hersen *et al*., 2004, Elberlrhiti *et al*., 2007, Baas, 2008, Duran *et al*., 2010, Zhang *et al*., 2012, Ping *et al*., 2014).

From streamer mode in barchan field to roll-over mode in barchanoid field: When sand supply increases in a barchan, e.g., when it travels on a sandy plain, or when the dune height and width increase through amalgamation of some neighbouring edifices, the output flux along the horn tips becomes more unequal to the input flux along the windward base, than in the case of small dunes. So, more sand gets trapped in the dune than is flushed out. As sand influx increases, the streamer mode of transport gets replaced by a roll-over mode. This may lead to horn tips becoming wider and blunt, crest and brink higher, and avalanching of sand along slip face more prominent, which may lead to the development of a new 'cone' (or 'tongue') of sand accumulation at the base of the slip face, and a reduction in the celerity of the dune. This generally happens in a field where the barchans are closely spaced and wind energy is high. It gradually leads to the formation of compound barchans or barchanoids where several dunes are joined along their horns (e.g., near Sam, Dhanana, Shagarh and other places to the SW of Jaisalmer). As the tongue at the base of slip face of individual crescentic bedforms grows in successive barchans along a chain, they join the barchans along their back also, giving an impression of over-riding bedforms (a gridiron pattern).

From barchans to linear dunes in Thar Desert: Observations and new learning

Observations and postulates: One problem that we faced in western Thar way back in the 1980s was in agreeing to the then-prevailing theory of evolution of linear dunes from parabolic dunes, as proposed by Verstappen (1968, 1970). Most researchers in other deserts had till then reported linear dune formation under a bi-directional wind system, with characteristic "sief" (sword's edge) along the dune crest and a distinctly sinuous pattern (Lancaster, 1980; Tsoar, 1983, 1984). Years of our observations in field and on aerial photographs of the mobility and growth of barchan and linear dunes in western Thar convinced us that the linear dunes in our desert did not develop from parabolic dunes, nor did they have any 'seif' shape of the crest with slip face alternating along the dune.

Based on our observations we proposed that the linear dunes in western Thar develop from streams of barchans. The barchans first colonize narrow strips of land under a strong unidirectional wind, and then gradually get linked along their horns and back in the manner sketched in the earlier section, and their interdune spaces get filled up while the crestal part maintains a crescentic form in response to high wind (Kar, 1987). If one moves across any such densely colonized and linked gridiron-patterned barchanoids, especially along the crestal segment, one gradually reaches higher ground as one moves

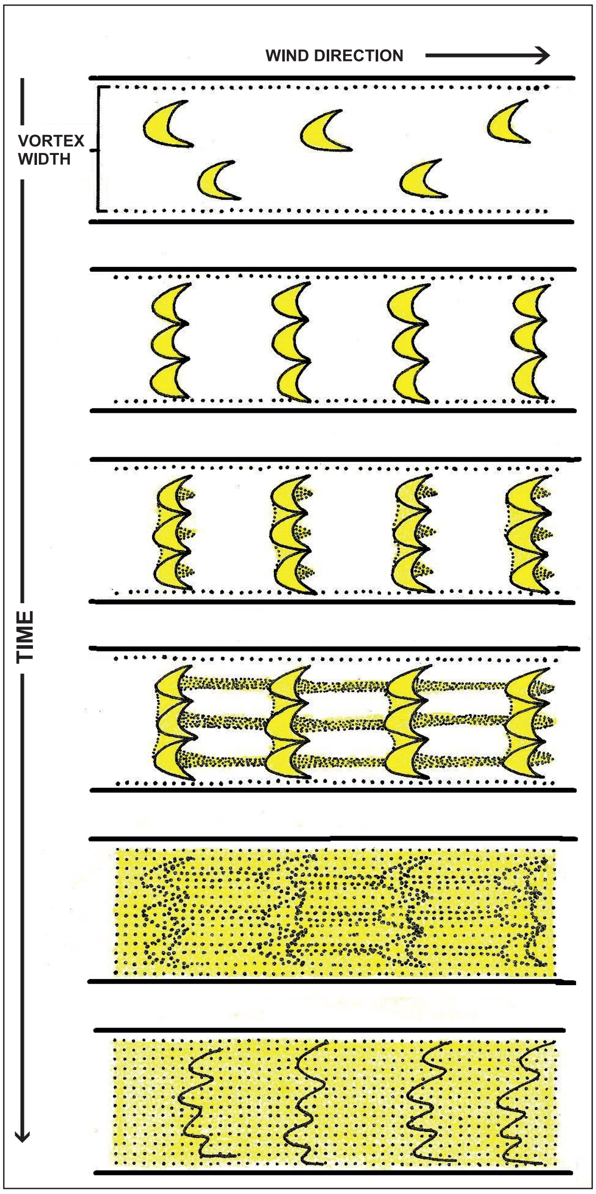

Fig. 9. A scheme for the evolution of linear dunes from streams of barchans to the W of Jaisalmer (after Kar, 1987).

from side to the middle part of a dune cluster. The peaks occur along the central axis of the colonized strip, where wind speed and sand transport rates are also higher. Gradually these linearly-arranged crescentic bedforms assume a smoother convex crest as stabilization process sets in, and ultimately produce the broadly-convex linear dunes (Fig. 9).

We also found that the large megabarchanoid fields to the SW of Jaisalmer and adjoining Tharparkar area of Pakistan, which get supplies from and grow at the expense of old linear dunes in the area (i.e., within GP-17 of Fig. 1), follow a development path almost identical to the barchan-to-linear dune growth sequence (Kar, 1990). Our observations on stages of linear dune development helped researchers to re-think about earlier views on linear dune development (Pye and Tsoar, 1990, Cooke et al., 1993, Lancaster, 1995). Reports of identical pattern of linear dune growth from linked barchans elsewhere on Earth and other planets, however, came only recently (Bourk and Goudie, 2009), especially as high-resolution space images, like from Google Earth, Cassini, or Mars Odyssey, became available. These new findings may encourage researchers in other deserts to test the barchan-to-linear dune growth sequence suggested by us.

Role of atmospheric boundary layer: Bagnold (1941) had suggested that linear dunes in the Sahara might have originated due to strong thermal convection over desert plains that generated roll-vortices carrying the sand downwind along defined narrow lanes. Several studies since then investigated the causal relationship between aeolian bedforms and atmospheric boundary layer (ABL). Hanna (1969), based on laboratory simulation results and numerical studies, suggested the formation of counter-rotating helical roll vortices aligned along the wind and having a wavelength of approximately 3 times the thickness of ABL, when Reynolds number reached a value of about 115-125, and deposition of sand along their convergence for linear dune formation at wavelengths determined by the vortices. His hypothesis has no taker now, but it generated renewed interest on investigating the link with ABL (e.g., Wilson, 1972; Tseo, 1993). Wilson (1972) suggested that some pairs of longitudinal spiral vortices might pre-exist in the flow and some might be induced by bedform irregularities, but in both cases the particles are picked up or carried from their points of attachment and deposited along the points of separation. He also postulated the existence of some transverse wave motion in sheared thermal turbulence which might have formed the large transverse bedforms (draas), but like in the case of longitudinal vortices, smaller such elements can also be formed due to interaction between secondary flow and the developing bedform. According to him, both the longitudinal and transverse elements may occur as independent elements or in combination, producing different kinds of bedforms over time and space. Relating our results of linear dune wavelength and height in western Thar (average wavelength of >20 m high linear dunes being 0.8-1.0 km, while that of the <20 m high dunes being 0.25-5.0 km) with the above studies we presumed, following Wilson (1972), that the high thermal instability over the region during strong summer months formed narrow lanes of vortices at almost regular spacing, where alternate 'streets' became first populated with barchans. Gradually the closely-spaced and linked barchans were transformed into the tall linear dunes (Kar, 1987), although the precise mechanism remained to be understood.

New findings from ABL research: Results linking ABL with large-scale dune field development were doubted in field-based research since 1980s, especially as most measurements on single dunes in field failed to pick up enough evidence of the ABL-scale changes, and also as computer simulation modeling with ABL parameters was at a nascent stage (Livingstone *et al.*, 2007). The single-dune research, however, generated many quantified informations that helped in understanding the aeolian process-form interaction at micro-level. Partly based on those researches, new simulation modeling of small aeolian bedform development suggests that at individual field-scale, a feedback mechanism exists in the aeolian transport system such that once sand grains start moving they tend to modify the surface topography, which in turn modifies the flow, resulting in an array of bedform types, even under a dominantly unidirectional wind, but with changing influx-outflux ratios with time (Schwammle and Herrmann, 2005; Duran *et al.*, 2010). This process does not require any kind of atmospheric vortices to explain the sequence of bedform growth from single barchans to a linearly arranged array of coalesced barchans and their further modifications. Neither does it disprove the importance of atmospheric vortices in the development of dune fields, studies on which now provide good evidence of the influence of ABL in development of different types of sand dunes (Andreotti *et al.*, 2009; Weaver and Wiggs, 2011; Jerolmack *et al.*, 2012; Kok *et al.*, 2012).

Andreotti *et al.* (2009) showed that the giant desert dunes and the dunes in rivers are formed by similar processes, where the thermal inversion layer, capping the convective boundary layer (CBL) in atmosphere, acts analogously to the water surface in rivers, such that the bed topography excites surface waves on the interface that in turn modify the near-bed flow velocity. In the absence of direct measurement of ABL conditions, they used the seasonal variations in potential temperature near the ground and the potential lapse rate as surrogates, and then discussed how the small-amplitude dunes grow and coarsen until they are limited by the thickness of the thermal inversion layer that caps the convective boundary layer (CBL) in the atmosphere. The mechanism, according to the authors, can explain the mean spacing of dunes from 300 m to 3.5 km.

Another significant study has shown that as the strong summer wind approaches an existing bedform-cluster (e.g., linearly arranged barchanoids) over the desert plain, it encounters an abrupt increase in surface wind stress at the upwind end of the dune field. This is followed by gradual development of an internal boundary layer that thickens downwind and causes a decline in wind stress as well as sediment flux in that direction, as was estimated from LiDAR topographic mapping in New Mexico, USA, where the transition is from a field of bare barchanoids to that of vegetated parabolic dunes. The correlation between sand flux and shear stress above threshold improves over a long timescale (Jerolmack *et al.*, 2012; Martin *et al.*, 2013). The basic ideas behind the above findings are in broad agreement with the long-held postulates from flume-based research in sedimentology and from fluid dynamics (now called computational fluid dynamics, CFD), which now form important component of a growing body of complex research to understand patterns in the nonlinear and non-equilibrium dynamical earth systems. Such multi-disciplinary research, involving different fields, can address several issues from a different perspective (Goehring, 2013).

Surface temperature, CBL and dune fields in the Thar: The above findings are important for Thar Desert, where we find clusters of tall linear, transverse or parabolic dunes with near-uniform wavelengths within a dune field. Smaller dunes do also exist within the dune fields and have different wavelengths. Our earlier view, based on Wilson's (1972) suggestion that the old linear dunes in the west might have formed due to thermal instability involving the ABL, do get vindicated by the new research. Interestingly, we observed from field measurements across barchan topography not only high near-surface temperature during the summer, but also a large difference between the air and the 'skin' temperature of the dune (13-21^{o}C at different locations on the dunes on measurement days), as also high diurnal range of temperature (13-26^{o}C, the range being smaller during May-June, and on the crest; Ramakrishna *et al.*, 1990, 1994). Our limited study over a barchan and a parabolic dune at Shergarh also showed that the summer time convective turbulence, as measured through Richardson number (Ri), varied between -7.5 and -17.1, the higher turbulence being recorded at the dune crest (Ramakrishna *et al.*, 1990). Commonly, an atmospheric layer is considered 'stable' with laminar flow at Ri >1.0; turbulent due to mechanical shear at 0 <Ri <0.25; convectively unstable at Ri <0; and maintaining current state, whether laminar or turbulent at 0.25 <Ri <1.0. Although a full understanding of the atmospheric physics in calculation of Ri and its evolution is beyond the scope of our subject, the Ri scale for measuring turbulence is important for linkage with the overall aeolian process parameters.

Perusal of the MODIS satellite data on land surface temperature about 1 m above the surface (MOD11A2, 1 km pixel, 8-day summaries, clear sky days; basic data sourced from LP_DAAC, USGS) for March to early June, 2001-2010, showed that at regional scale the mean maximum day temperature was over the linear dune field with megabarchanoids (GP-17), especially during April and May, when the mean hovers around 48-50^{o}C. For the desert

Table 4. Average day-time near-surface air temperature (ºC; approx. 1 m above surface) over different geomorphic provinces during March to mid-June, 2001-2010, as calculated from MODIS satellite data at 1 km resolution (8-day summary)

	D-65*	D-73	D-81	D-89	D-97	D-105	D-113	D-121	D-129	D-137	D-145	D-153
1#	37	40	42	43	45	46	47	47	44	46	46	45
2	29	32	36	37	41	43	46	46	47	48	47	47
3	34	37	40	41	43	44	47	47	47	48	43	44
4	37	40	43	43	46	46	46	47	45	48	43	45
5	40	43	45	46	47	48	46	49	48	47	45	46
6	40	43	45	45	46	47	49	48	45	44	44	43
7	38	41	43	44	46	47	49	47	47	44	45	44
8	39	42	44	45	47	48	50	48	48	46	45	43
9	38	42	43	43	46	47	47	47	46	45	45	41
10	40	42	44	45	46	47	48	47	46	44	44	42
11	41	44	46	46	48	48	50	49	47	46	45	43
12	40	44	46	46	47	47	49	48	45	45	44	42
13	35	37	40	41	44	45	46	44	47	49	46	46
14	39	41	44	45	47	47	50	48	49	49	47	47
15	35	37	39	40	41	43	45	44	46	46	46	44
16	38	40	43	44	46	47	49	48	49	49	49	47
17	41	44	46	46	48	49	50	49	49	48	48	45

Geomorphic province code, as in Table 1; * D denotes Julian day; associated number denotes the first day of the 8-day period (i.e., D-65 is 06-13 March for non-Leap year; 5-12 March for Leap year; D-73 is 14-21 March for non-Leap year, etc.).

as a whole, the mean day temperature across the geomorphic provinces during March-May varied between 40ºC and 48ºC (Table 4). Such high near-surface temperature should lead to high turbulences in the ABL.

To find out if the spatio-temporal pattern of strong near-surface turbulence at dune field scale varies with the concentration of crescentic bedforms (i.e., barchans and megabarchanoids) in our desert, as well as with the sand/dust emission potential, we mapped the mean monthly Ri values for March to July (2001-2010) over the region (Fig. 10). The Ri data was sourced from NASA-Giovanni's Modern Era Retrospective-analysis for Research and Applications (MERRA) site, and processed in GIS. Mapping reveals that by March a strong convective turbulence layer (CBL) develops over GP-17 (mean Ri -0.41), when large parts of the desert start experiencing variable turbulence, except in the northern plains (GP-2) that still remain mostly unaffected. Within GP-17 the stronger mean Ri exceeding -0.60 is noticed within the core area of megabarchanoid fields. By April the mean Ri over GP-17 intensifies beyond -0.5 and the area expands linearly across GP-9 and GP-8 (i.e., through Jaisalmer and Ramgarh to the vicinity of Bahla, Bikampur and Bijnot), where the maximum negative values go beyond -0.65. By May the convective turbulence in the megabarchanoid core area exceeds -0.75 (as also in GP-14 and GP-16), while the high convective turbulence represented by mean Ri of -0.51 to -0.70 expands to almost the whole area to the west of a line joining Jaisalmer, Bikaner and Churu. By June, Ri improves slightly in SW Thar, including GP-17, but the values decline below -0.65 in NW Thar, especially to the west of Tanot-Bikaner-Churu line. As expected, Ri improves across the desert further during July, but a zone roughly between Ramgarh, Nachna, Bikampur, Pugal, Derawar Fort and Islamgarh still experiences higher turbulence (Ri <-0.55). Vertically, the CBL appears to extend up to 800 hPa (approximately 1900 m) during the summer months. When viewed with wind speed during the period, the Ri distribution pattern helps

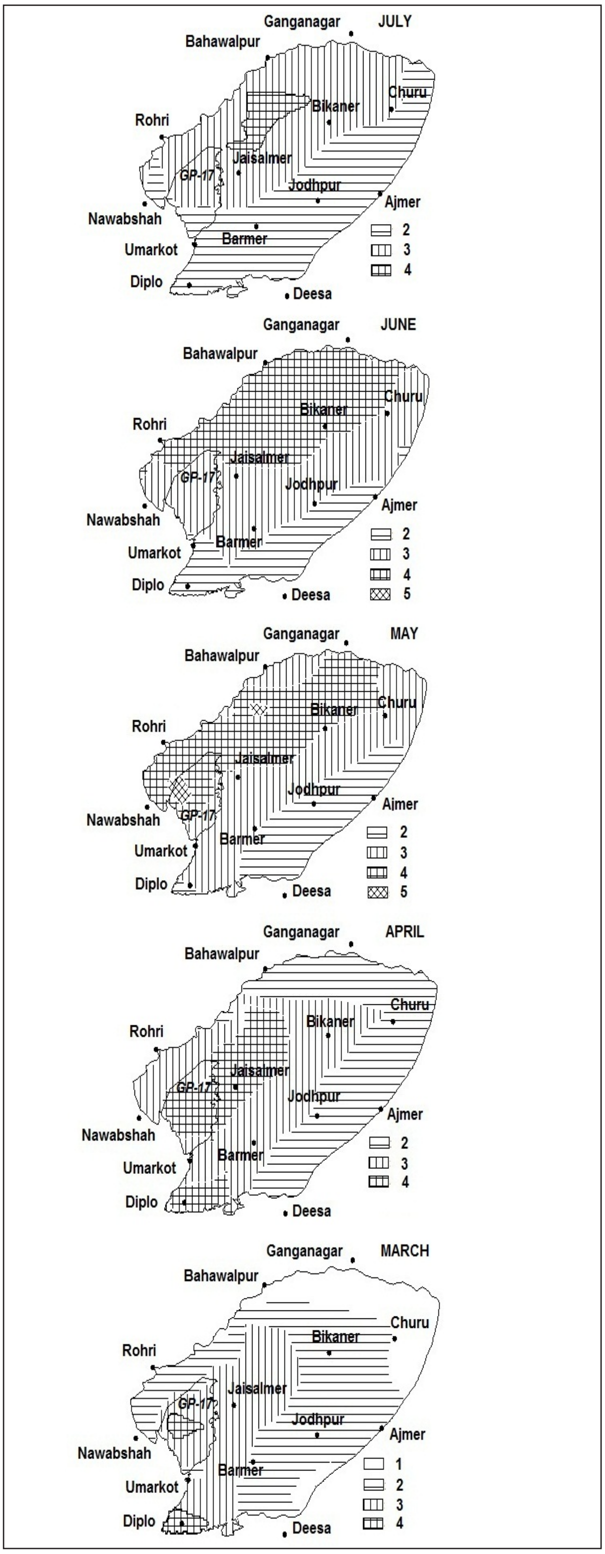

Fig. 10. Classification map of mean Surface Richardson Numbers (Ri) for Thar Desert (March, April, May, June and July), averaged from the values for 2001 to 2010. Legend: 1= 0.25 to 0.0; 2= -0.01 to -0.30; 3= -0.31 to -0.50; 4= -0.51 to -0.70; 5= -0.71 to -0.90.

us to visualize the expected pattern of sand reactivation and sand/dust emission across the desert. It also matches well with the strong presence of megabarchanoids in GP-17.

The growing evidence for CBL control on sand flow during periods of strong wind make us wonder if the eastward fall in the level of summer-time turbulence in the Thar, along with declining wind speed in that direction, can partly explain the gradational contact of the linear dune field with the parabolic dune field to its east. As we have discussed earlier, parabolic dunes are formed to the east of the linear dune field in a gradually lower wind environment and with higher sand availability (i.e., GP-11). The transition from the 10-12 km long unattached individual linear dunes, oriented SSW-NNE (occasionally with short feathers on western flank) in the extreme west of the desert, to inverted Y-junctioned ones eastward, and then to clusters of 5-8 linear dunes converging at an acute angle without much downwind progress, followed first by long-arm hairpin parabolic dunes and then short-arm parabolic dunes further east, with progressive change in dune direction from N77ºE in the west to N48º-50ºE in the east, appear to be a distinct adjustment of the dunes to a gradual change in velocity and directional variability of wind eastward (Kar, 1993). As wind becomes more feeble further east, the parabolic dunes start to disintegrate into hooked dunes and other forms of network dunes (GP-4).

We have argued earlier (Kar, 1996) that the parabolic dunes in our desert did not develop due to anchorage and elongation of arms by vegetation and deflation of plains in between, but through a process that is independent of such control. We have noticed in several parabolic dune fields that sand accumulation downwind of an existing old parabolic dune takes place first as isolated depositional lobes that become joined with time to form two linear sand streaks. Simultaneously another lobe develops further downwind, which grows as the curved nosal segment of the parabolic bedform; the linear streaks join the nose to form two arms of the new parabolic dune. While this growth sequence is a result of wind and sand flow pattern dictated by the old parabolic dune upwind, it also hints at the possibility of some CBL-level assistance.

Allen (1985) found evidence that a low-level vortex of certain width astride the path of wind, and moving in the direction of wind as a straight barrel, carrying sand along a low streak, gradually transforms into a broadly parabola-shaped vortex further downwind as it moves forward with increased sand load and higher wind speed. Further downwind it takes a hairpin parabolic shape with acute angle bend, when the nosal part of the vortex buoys up significantly as the bedform height and the wind speed above ground also increases. Ultimately, this upwardly bent, sand-laden hairpin vortex becomes very unstable and bursts (streak bursting), ejecting the sand load at that point. The wind re-groups again downwind to re-start the process. Consequently, the linear ridges below such vortex should show peaks at certain intervals, as is noticed along the linear dunes. If such vortices develop in pairs in areas of falling wind speed and weaker turbulence, they may result in the development of two arms of a parabolic dune and a nose at the site of streak bursting. With the rapid development in CFD research, reasons for eastward change in dune shape from the linear to the long-arm hairpin parabolic to the short-arm parabolic and then to the hooked dunes and disjointed large parabolic plan-form with network within, could perhaps be obtained soon.

From Site-based Estimates to Regional-scale Assessment: The Way Forward

Although field measurements have provided us important understanding of the aeolian process-form interaction at individual bedform-level, the high variability of landscape elements in the desert, especially in terms of bedform types and distribution, sediment characteristics, vegetation component, soil moisture, etc., as well as the variability in wind regime, make the quantification of few parameters in small dune-scale studies less relevant for local to regional scale assessment. A broader view of the different biophysical parameters at play and attempts to link them becomes necessary. As human activities have now become a major driving force in accelerating the geomorphic processes faster than the geological rates, and in changing the geomorphic features in a way never before, especially through drastic land use changes and mechanization of agriculture, the roughness density, the shear stress and the erodibility of the aeolian landscape are changing fast, with immense consequences for grain transport, sand/dust emission and bedform mobility during the dry and windy summer months. Focusing on the bio-physical aspects alone, therefore, has also become inadequate, and has necessitated the simultaneous interpretation of socio-economic variables that increase the pressure of certain kinds, and link the results with the biophysical dataset in GIS for a purposeful interpretation of the aeolian dynamics. This calls for an integrated understanding of the aeolian science across many fields. It is now increasingly felt by the global research communities that the reductionist view of highly compartmentalized component research should give way to a non-reductionist and holistic approach with equal or more emphasis on the system components (Thomas and Wiggs, 2008).

Remote sensing provides now a wide range of data on many landscape elements and atmospheric variables at different spatio-temporal scales, the analysis of which help us to integrate many of the forms and processes for a holistic understanding of the system dynamics. The MODIS land surface temperature data (Table 4), or the processed Ri data are just small examples of the huge global data from satellite sensors and ground observations that are being regularly ingested, processed and then supplied to researchers. Since the data are available as pixels of certain resolution, the images on different parameters can be linked to gridded data from different sources, including the socio-economic data, in a GIS framework for calculation of aeolian system response to perturbations. For example, in the southern part of Churu District we calculated the Color Brightness Index (CBI) of the sandy terrain from Landsat MSS (1973) and ETM (2001) image data, using Mathieu *et al*. (1998) formulae, and density-sliced the values based on ground truth to classify the degree of sand reactivation. It separated the areas of riverine sand, the salt-encrusted surfaces and the gypsiferous interdunes from the reactivated aeolian sand very well, and showed that in 2001 about 52% of the total area had increased reactivation than in 1973, 12% area had lesser reactivation, and 36% had no change. We then carried out an analysis of cropland and rangeland uses in the area, and co-evaluated the results with CBI at pixel level to find out the apparent driving forces for increased sand reactivation. It revealed a higher correlation between cropland use intensity with CBI, than between rangeland use and CBI, suggesting that activities like destruction of natural vegetation and deep ploughing through tractors that are associated with modern cropland uses through groundwater irrigation, were more responsible for increased sand reactivation than open grazing of already depleted rangeland resources by the livestock (Kar, 2011).

The analysis, however, did not work well when applied to the desert as a whole, because the signatures from silt-rich sediments, especially in the north-western part, got mixed with the signatures of reactivated aeolian sand in that part. In order to minimize this potential source of error, we applied another index called the 'grain-size index' (GSI) that was successfully applied in the Mongolian Desert (Xiao *et al*., 2006). We found that GSI could largely discriminate the fine aeolian sand (bright) from the silt-clay-rich sediments (dull). Sparsely vegetated gravel plains that also were bright in CBI, could also be separated due to its dullness in GSI. Merging the CBI with GSI and re-calibration of the reactivation index helped to classify the sand-reactivated areas more confidently over large parts, but a trade-off was still present between the selection of grain size and reactivation category. This is being refined.

The partial success in manipulating the surface reflectance values for sand reactivation categories has opened the possibility of using remote sensing products for regional-scale quantification and mapping of sand flux with and without plant cover, and a host of other applications. If GSI values can be used to faithfully reflect the mean or median grain sizes at surface, and if plant cover during summer months could be adequately quantified in terms of density and height (including for the senescent small shrubs in a sandy plain or over a dune), a realistic quantification of regional-scale sand transportation over time and space can be possible with the use of high-resolution DEMs and gridded meteorological data. This may help in better understanding of the patterns of degradation of the aeolian landscape and rates of dune movement, as well as in bridging crucial gaps in the budgeting of sand/dust emission, transportation and deposition.

Several satellite sensors are regularly monitoring the atmospheric dust load over the earth since 1979, especially as aerosol index (AI) and aerosol optical depth (AOD). Using data from observation towers and simulation modeling, several attempts have also been made to convert the AI and AOD into actual dust load quantities (Tegen and Funk, 1994; Marticorena *et al*., 1997; Goudie and Middleton, 2006; Prasad *et al*., 2006; Gautam *et al*., 2009; Shao *et al*., 2011). Our limited studies have shown that the variability in wind erosion index (WEI; Kar, 1993) may be used as a proxy for AI variability under natural settings, and that it can be used to predict the likely atmospheric dust loads, and hence the pattern of sand reactivation and mobilization of sand dunes and sandy plains during the periods when sensor-based AI data was not available. The index was also used to calculate the likely pattern of sand reactivation during 21st Century under the GCM-predicted climate, which suggested that the wind erosion and atmospheric dust load would most likely increase manifold between 2016 and 2030, followed by several high-magnitude changes till the end of the century (Kar, 2012). Using a different 'dune mobility index' Thomas *et al*. (2005) suggested significant enhancement of dune activity in the Kalahari Desert by 2039 and 2069.

It is expected that remote-sensing-driven quantification of land surface and atmospheric parameters at pixel level and their integrated analysis in GIS will soon provide us with actual quantities of sand/dust being emitted, transported and deposited during each phase of surface reactivation, while identification of drivers of sand/dust emission and quantification of their pressure will help to address the losses due to degradation in a region. As human activities through land use modifications and mechanization have started to make large-scale land surface changes through land use modifications, the previously-held area-averaged thresholds of erosion for the surfaces have become more patchy, the calculated WEI have become less relevant, and the long-term rates of change under natural setting have started to get surpassed over a large area. Quantification of drivers and their pressures, therefore, assume a higher importance in the modeling efforts.

Conclusions

Research during the last few decades has led to modest gains in our knowledge of the aeolian bedforms and processes in Thar Desert, especially as quantification was carried out mostly in field, and to the extent possible despite logistic constraints. Those in-depth, site-based studies on single dunes and small areas helped us to test the fundamental principles of aeolian bedform perturbation, and to intuitively work out the likely interaction between forms and processes over the vast desert terrain. Collation of the results and interpretation of the data, however, show some inadequacy in their use for a proper regional-scale assessment, as the data points are severely limited compared to the immense variability of the landscape.

As data on many different aspects of the forms and processes are now becoming available from high-resolution satellite sensors and new insights are provided from 3-D rendering of the surface and atmospheric variables, confidence on the fundamental equations are growing, and new computational power of CFD and GIS applications are getting manifested. A paradigm shift has already started in our approach to the aeolian research. While the focus so far was on small sites, single dunes and often compartmental research, the new studies are region-wide and multi-disciplinary, with an emphasis on the holistic view of landscape or the problem. It is now increasingly felt that the new integrative research in earth system dynamics, which accepts that both biophysical sciences and social sciences are equally important in understanding the earth's present and future dynamics, should replace the compartmental research. This new development does not preclude field-based research, but shows how a limited number of field sites and instrumentation could be decided upon from the regional-scale data for calibrating the acquired data, and for additional computational purposes. As we have discussed in this paper, such shifts in approach to aeolian research has already taken place in the context of many global deserts as well as for understanding extra-terrestrial aeolian processes.

To herald in the new-era research for Thar Desert, our review shows the need for developing a robust spatio-temporal database on all the relevant geomorphic variables, and also adequate database on complementary fields. Digital remote sensing, when used in the right kind of physical models and with all the relevant time-varying information on meteorological, topographic, granulometric, hydro-edaphic and land use aspects, as well as on barrier types, etc., can provide somewhat reliable information. The complexity of the problems and challenges thrown up by the use of the sandy terrain, though, makes it still difficult for us to arrive at any universally acceptable package of solution to the problems.

One feels that geomorphologists are better trained to become what Sherman (1996) calls a "fashion leader" to evaluate and accept the new paradigms of aeolian research discussed above, as well as to adopt some radical new thoughts and approaches developed in other complementary fields. One hopes that such dynamic "fashion leaders" will be able to motivate others in a multi-disciplinary aeolian research group to not only change track for better understanding of the system dynamics, but also to encourage the use of results for social good.

References

Ahlbrandt, T.S. 1979. Textural parameters of eolian deposits. In *A Study of Global Sand Seas* (Ed. E.D. McKee), pp. 21-51. USGS Professional Paper 1052.

Allen, J.R.L. 1985. *Principles of Physical Sedimentology*. George Allen and Unwin, London, 272 p.

Andreotti, B., Fourriere, A., Ould-Kaddour, F., Murray, B. and Claudin, P. 2009. Giant aeolian dune size determined by the average depth of the atmospheric boundary layer. *Nature* 457: 1120-1123.

Baas, A.C.W. 2008. Challenges in aeolian geomorphology: Investigating aeolian streamers. *Geomorphology* 93: 3-16.

Bagnold, R.A. 1941. *The Physics of Blown Sand and Desert Dunes*. Methuen, London, 265 p.

Barndorff-Nielsen, O., Dalsgaard, K., Halgreen, C., Kuhlman, H., Moller, J.T. and Schou, G. 1982. Variation in particle size distribution over a small dune. *Sedimentology* 29: 53-65.

Bourke, M. and Goudie, A.S. 2009. Varieties of barchan form and the Namib Desert and on Mars. *Aeolian Research* 1: 45-54.

Buckley, R.C. 1987. The effect of sparse vegetation on the transport of dune sand by wind. *Nature* 325: 426-428.

Cooke, R., Warren, A. and Goudie, A. 1993. *Desert Geomorphology*. UCL Press, London.

Dhir, R.P. 2003. Thar Desert in retrospect and prospect. *Proceedings, Indian National Science Academy* 69A(2): 167-184.

Dhir, R.P., Singhvi, A.K., Andrews, J.E., Kar, A., Sareen, B.K., Tandon, S.K., Kailath, A. and Thomas, J.V. 2010. Multiple episodes of aggradation and calcrete formation in Late Quaternary aeolian sands, Central Thar Desert, Rajasthan, India. *Journal of Asian Earth Sciences* 37: 10-16.

Dong, Z., Liu, X., Wang, H. and Wang, X. 2003. Aeolian sand transport: A wind tunnel model. *Sedimentary Geology* 161: 71-83.

Duran, O., Parteli, E.J.R. and Herrmann, H.J. 2010. A continuous model for sand dunes: Review, new developments and application to barchan dunes and barchan dune fields. *Earth Surface Processes and Landforms* 35: 1591-1600.

Elbelrhiti, H., Andreotti, B. and Claudin, P. 2008. Barchan dune corridors: Field characterization and investigation of control parameters. *Journal of Geophysical Research* 113(F02S15): 1-21.

Folk, R.L. 1971. Genesis of longitudinal and oghurd dunes elucidated by rolling upon grease. *Geological Society of America Bulletin* 82: 3461-3468.

Folk, R.L. and Ward, W.C. 1957. Brazos river bar: A study in the significance of grain-size parameters. *Journal of Sedimentary Petrology* 27: 3-27.

Gautam, R., Hsu, N.C., lau, K-M. and Kafatos, M. 2009. Aerosol and rainfall variability over the Indian monsoon region: Distributions, trends and coupling. *Annales Geophysicae* 27: 3691-3703.

Ghose, B., Kar, A. and Husain, Z. 1979. The lost courses of the Saraswati river in the Great Indian Desert: New evidence from Landsat imagery. *Geographical Journal* 145: 446-451.

Ghose, B., Singh, S. and Kar, A. 1977. Desertification around the Thar: A geomorphological interpretation. *Annals of Arid Zone* 16: 290-301.

Goehring, L. 2013. Pattern formation in the geosciences. *Philosophical Transactions of the Royal Society* A 371: 1-7.

Goudie, A.S. and Middleton, N.J. 2006. *Desert Dust in the Global System*. Springer, 287 p.

Goudie, A.S., Allchin, B. and Hegde, K.T.M. 1973. The former extensions of the Great Indian Sand Desert. *Geographical Journal* 139: 243-257.

Gupta, J.P. 1993. Wind erosion of soils in drought prone areas. In, *Desertification in Thar, Sahara and Sahel Regions* (Eds., A.K. Sen and A. Kar), pp. 91-105. Scientific Publishers, Jodhpur.

Hanna, S.R. 1969. The formation of longitudinal sand dunes by large helical eddies in the atmosphere. *Journal of Applied Meteorology* 8: 874-883.

Hersen, P., Andersen, K.H., Elbelrhiti, H., Andreotti, B., Claudin, P. and Douady, S. 2004. Corridors of barchan dunes: Stability and size selection. *Physical Review E: Statistical, Nonlinear and Soft Matter Physics* 69: 113041-1130412.

Jaswal, A.K. and Koppar, A.L. 2013. Climatology and trends in near-surface wind speed over India during 1961-2008. *Mausam* 64: 417-436.

Jerolmack, D.J., Ewing, R.C., Falcini, F., Martin, R.L., Masteller, C., Phillips, C., Reitz, M.D. and Buynevich, I. 2012. Internal boundary layer model for the evolution of desert dune fields. *Nature Geoscience* 5: 206-209.

Juyal, N., Kar, A., Rajaguru, S.N. and Singhvi, A.K. 2003. Luminescence chronology of aeolian deposition during the Late Quaternary on the southern margin of Thar Desert, India. *Quaternary International* 104: 87-98.

Kar, A. 1987. Origin and transformation of longitudinal sand dunes in the Indian desert. *Zeitschriftt fur Geomorphologie* 31: 311-337.

Kar, A. 1990. The megabarchanoids of the Thar: Their environment, morphology and relationship with longitudinal dunes. *Geographical Journal* 156: 51-61.

Kar, A. 1993. Aeolian processes and bedforms in the Thar Desert. *Journal of Arid Environments* 25: 83-96.

Kar, A. 1994. Sand dunes and their mobility in Jaisalmer district. In, *India - Geomorphological Diversity* (Eds. K.R. Dikshit, V.S. Kale and M.N. Kaul), pp. 395-418. Rawat Publishers, Jaipur.

Kar, A. 1995. Geomorphology of arid western India. *Memoir, Geological Society of India* 32: 168-190.

Kar, A. 1996. Morphology and evolution of sand dunes in the Thar Desert as key to sand control measures. *Indian Journal of Geomorphology* 1: 177-206.

Kar, A. 1999. Cluster analysis of grain size information for possible linkages between geomorphic environments: Some case studies from Indian arid zone. *Zeitschrift fur Geomorphologie* 43: 27-39.

Kar, A. 2002. Granulometry of aeolian bedforms in the extremely arid Jaisalmer region of Thar Desert. In *Recent Advances in Geomorphology, Quaternary Geology and Environmental Geosciences: Indian Case Studies* (Eds. S.K. Tandon and B. Thakur), pp. 261-286. Manisha Publications, New Delhi.

Kar, A. 2009. An analysis of climate change through quantification of forms and processes in the Thar Desert. In *Earth System Sciences*, (Eds. A. Kumar, R.A. Kushwaha, and B. Thakur), Vol. 2, pp. 363-381. Concept Publishing Co., New Delhi.

Kar, A. 2011. Geoinformatics in spatial and temporal analysis of wind erosion in Thar Desert. In *Geoinformatics in Applied Geomorphology* (Eds. S. Anbazhagan, S.K. Subramanian and X. Yang), pp. 39-62. CRC Press, Boca Raton, USA.

Kar, A. 2012. GCM-derived future climate of arid western India and implications for land degradation. *Annals of Arid Zone* 51: 147-169.

Kar, A. 2013. Quaternary geomorphic processes and landform development in the Thar Desert of Rajasthan. In *Landforms Processes and Environment Management* (Eds. S. Bandyopadhyay, M. Bhattacharji, S. Chaudhuri, D.C. Goswami, S.R. Jog and A. Kar), pp. 225-256. ACB Publications, Kolkata (revised reprint).

Kar, A. 2014. The Thar or the Great Indian Sand Desert. In, *Landscapes and Landforms of India* (Ed. V.S. Kale), pp. 79-90. World Geomorphological Landscapes Series, Springer, Dordrecht.

Kar, A. and Ghosh, B. 1984. Drishadvati River system in India: An assessment and new findings. *Geographical Journal* 150:221-229.

Kar, A., Felix, C., Rajaguru, S.N. and Singhvi, A.K. 1998. Late Holocene growth and mobility of a transverse dune in the Thar Desert. *Journal of Arid Environments* 38: 175-185.

Kar, A., Singhvi, A.K., Juyal, N. and Rajaguru, S.N. 2004. Late Quaternary aeolian sedimentation history of the Thar Desert. In *Geomorphology and Environment* (Eds. H.S. Sharma, Savindra Singh and Sunil De), pp. 105-122. ACB Publications, Kolkata.

Kar, A., Singhvi, A.K., Rajaguru, S.N., Juyal, N., Thomas, J.V., Banerjee, D. and Dhir, R.P. 2001. Reconstruction of the late Quaternary environment of the lower Luni plains, Thar Desert, India. *Journal of Quaternary Science* 16: 61-68.

Kok, J.F., Parteli, E.J.R., Michaels, T.I. and Bou-Karam, D. 2012. The physics of wind blown sand and dust. *Reports on Progress in Physics* 75(10): 1-119.

Lancaster, N. 1980. The formation of seif dunes from barchans - supporting evidence for Bagnold's hypothesis from the Namib Desert. *Zeitschrift fur Geomorphologie* 24: 160-167.

Lancaster, N. 1995. *Geomorphology of Desert Dunes*. Routledge Press, London.

Lettau, H.H. and Lettau, K. (Eds.) 1978. *Exploring the World's Driest Climate*. IES Report 101, Center for Climatic Research, University of Wisconsin-Madison, Madison, 264 p.

Lettau, K. and Lettau, H. 1969. Bulk transport of sand by the barchans of the Pampa de La Joya in southern Peru. *Zeitschrift fur Geomorphologie* 13: 182-195.

Livingstone, I., Wiggs, G.F.S. and Weaver, C.M. 2007. Geomorphology of desert sand dunes: A review of recent progress. *Earth Science Reviews* 80: 239-257.

Marticorena, B., Bergmetti, G., Aumont, B., Callot, Y., N'Doume, C. and Legrand, M. 1997. Modeling the atmospheric dust cycle: 2. Simulation of Saharan dust sources. *Journal of Geophysical Research* 102D: 4387-4404.

Martin, R.L., Barcchyn, T.E., Hugenholtz, C.H. and Jerolmack, D.J. 2013. Timescale dependence of aeolian sand flux observations under atmospheric turbulence. *Journal of Geophysical Research, Atmospheres* 118: 1-15.

Mathieu, R., Pouget, M., Cervelle, B. and Escadafal, R. 1998. Relationships between satellite-based radiometric indices simulated using laboratory reflectance data and typic soil color of an arid environment. *Remote Sensing of Environment* 66: 17-28.

Moharana, P.C., Gaur, M.K., Chaudhary, C., Chauhan, J.S. and Rajpurohit, R.S. 2013. A system of geomorphological mapping for western Rajasthan with relevance for agricultural land use. *Annals of Arid Zone* 52(3&4): 165-182.

Naruse, T. 1985. Aeolian geomorphology of the Punjab plains and the north Indian desert. *Annals of Arid Zone* 24: 267-285.

Okin, G.S. 2013. Linked aeolian – vegetation systems. In *Treatise on Geomorphology*, Vol.11, Aeolian Geomorphology Treatise on Geomorphology (Eds. J. Shroder, N. Lancaster, D.J. Sherman and A.C.W. Bass), pp. 428-439. Academic Press, San Diego.

Ping, L., Narteau, C., Dong, Z., Zhang, Z. and du Pont, S.C. 2014. Emergence of oblique dunes in a landscape-scale experiment. *Nature Geoscience* 7: 99-103.

Prasad, A.K., Singh, R.P. and Singh, A. 2006. Seasonal climatology of aerosol optical depth over the Indian subcontinent: Trend and departures in recent years. *International Journal of Remote Sensing* 27: 2323-2329.

Pye, K. and Tsoar, H. 1990. *Aeolian Sand and Sand Dunes*. Unwin Hyman, London.

Raina, P. 1992. Influence of sandy soil degradation on the fertility status. *Current Agriculture* 16: 45-54.

Ramakrishna, Y.S., Kar, A., Rao, A.S. and Singh, R.S. 1994. Micro-climate and mobility of a barchan dune in the Thar Desert. *Annals of Arid Zone* 33: 203-214.

Ramakrishna, Y.S., Rao, A.S., Singh, R.S., Kar, A. and Singh, S. 1990. Moisture, thermal and wind measurements over two selected stable and unstable sand dunes in the Indian Desert. *Journal of Arid Environment*s 19: 25-38.

Santra, P., Mertia, R.S. and Kushawa, H.L. 2010. A new wind-erosion sampler for monitoring dust-storm events in the Indian Thar Desert. *Current Science* 99: 1061-1067.

Sarre, R.D. and Chancey, C.C. 1990. Size segregation during aeolian saltation on sand dunes. *Sedimentology* 37: 357-365.

Schwammle, V. and Herrmann, H.J. 2005. A model of barchan dunes including lateral shear stress. *European Physical Journal* E16: 57-65.

Shao, Y., Wyrwoll, K-H., Chappell, A., Huang, J., Lin, Z.,, McTainsh, G.H., Mikami, M., Tanaka, T.Y., Wang, X. and Yoon, S. 2011. Dust cycle: An emerging core theme in Earth system science. *Aeolian Research* 2: 181-204.

Sherman, D.I. 1996. Fashion in geomorphology. In *The Scientific Nature of Geomorphology* (Eds. B.L. Rhoads and C.E. Thorn), pp. 87-114. John Wiley & Sons.

Singh, D.V., Purohit, R.S., Mertia, R.S., Laxminarayan, Poonia, S. and Kar, A. 2011. *Agrometeorological Handbook of Jodhpur (1971-2010)*. CAZRI, Jodhpur, 110 p.

Tegen, I. and Fung, I. 1994. Modeling of mineral dust in the atmosphere: Sources, transport, and optical thickness. *Journal of Geophysical Research* 99D: 22897-22914.

Thomas, D.S.G. 1986. The response diagram and ancient desert sands - A note. *Zeitschrift fur Geomorphologie* 30: 363-369.

Thomas, D.S.G. 1988. Analysis of linear dune sediment-form relationships in the Kalahari dune desert. *Earth Surface Processes and Landforms* 13: 545-553.

Thomas, D.S.G. and Wiggs, G.F.S. 2008. Aeolian system responses to global changes: Challenges of scale, process and temporal integration. *Earth Surface Processes and Landforms* 33: 1396-1418.

Thomas, D.S.G., Knight, M. and Wiggs, G.F.S. 2005. Remobilization of southern African desert dune systems by twenty-first century global warmimg. *Nature* 435: 1218-1221.

Tseo, G. 1993. Two types of longitudinal dune fields and possible mechanisms for their development. *Earth Surface Processes and Landforms* 18: 627-643.

Tsoar, H. 1983. Dynamic processes acting on a longitudinal (seif) dune. *Sedimentology* 30: 567-578.

Tsoar, H. 1984. The formation of seif dunes from barchans - A discussion. *Zeitschrift fur Geomorphologie* 28: 99-103.

Vautard, R., Cattiaux, J., Yiou, P., Thepaut, J-N. and Ciais, P. 2010. Northern hemispheric stilling partly attributed to an increase in surface roughness. *Nature Geoscience* 3: 756-761.

Verstappen, H. Th. 1968. On the origins of longitudinal (seif) dunes. *Zeitschrift fur Geomorphologie* 12: 200-220.

Verstappen, H. Th. 1970. Aeolian geomorphology of the Thar Desert and palaeoclimates. *Zeitschrift fur Geomorphologie* Suppl. 10: 104-120.

Vincent, P.J. 1984. Partyicle size variation over a transverse dune in the Nafud as Sirr, central Saudi Arabia. *Journal of Arid Environments* 7: 329-336.

Warren, A. 1972. Observations on dunes and bimodal sands in the Tenere Desert. *Sedimentology* 19: 37-44.

Wasson, R.J. and Hyde, R. 1983. Factors determining desert dune types. *Nature* 304: 337-339.

Wasson, R.J. and Nanninga, P.M. 1986. Estimating wind transport of sand on vegetated surfaces. *Earth Surface Processes and Landforms* 11: 505-514.

Watson, A. 1989. Windflow characteristics and aeolian entrainment. In *Arid Zone Geomorphology* (Ed. D.S.G. Thomas), pp. 209-231. International Book Distributors, Dehra Dun.

Weaver, C.M. and Wiggs, G.F.S. 2011. Field measurements of mean and turbulent airflow over a barchan sand dune. *Geomorphology* 128: 32-41.

Wilson, I.G. 1971. Desert sandflow basins and a model for the development of ergs. *Geographical Journal* 137: 180-199.

Wilson, I.G. 1972. Aeolian bedforms-their development and origins. *Sedimentology* 19: 173-210.

Xiao, J., Shen, Y., Tateishi, R. and Bayaer, W. 2006. Development of a topsoil grain size index for monitoring desertification in arid land using remote sensing. *International Journal of Remote Sensing* 27: 2411-2422.

Zhang, D., Narteau, C., Rozier, O. and du Pont, S.C. 2012. Morphology and dynamics of star dunes from numerical modeling. *Nature Geoscience* 5: 463-467.

Zhao, Z., Luo, Y. and Jiang, Y. 2011. Is global wind declining? *Advances in Climate Change Research* 2: 225-228.

Printed in December 2014